

Deep Face Restoration: A Survey

TAO WANG, Nanjing University, China

KAIHAO ZHANG, Harbin Institute of Technology (Shenzhen), China

JIANKANG DENG, Imperial College London, UK

TONG LU, Nanjing University, China

WEI LIU, Tencent, China

STEFANOS ZAFEIRIOU, Imperial College London, UK

Face Restoration (FR) aims to restore High-Quality (HQ) faces from Low-Quality (LQ) input images, which is a domain-specific image restoration problem in the low-level computer vision area. The early face restoration methods mainly use statistical priors and degradation models, which are difficult to meet the requirements of real-world applications in practice. In recent years, face restoration has witnessed great progress after stepping into the deep learning era. However, there are few works to systematically study the deep learning based face restoration methods. Thus, in this paper, we provide a comprehensive survey of recent advances in deep learning techniques for face restoration. Specifically, we first summarize different problem formulations and analyze the characteristics of face images. Second, we discuss the challenges of face restoration. With regard to these challenges, we present a comprehensive review of recent FR methods, including prior-based methods and deep-learning methods. Then, we explore developed techniques in the task of FR covering network architectures, loss functions, and benchmark datasets. We also conduct a systematic benchmark evaluation on representative methods. Finally, we discuss the future directions including network designs, metrics, benchmark datasets, applications, *etc*. We also provide an open source repository for all the discussed methods, which is available at <https://github.com/TaoWangzj/Awesome-Face-Restoration>.

CCS Concepts: • Computing methodologies → Computational photography.

Additional Key Words and Phrases: Face restoration, Deep learning, Survey, Low-level vision, Facial prior

ACM Reference Format:

Tao Wang, Kaihao Zhang, Jiankang Deng, Tong Lu, Wei Liu, and Stefanos Zafeiriou. 2025. Deep Face Restoration: A Survey. *ACM Comput. Surv.* 1, 1 (August 2025), 35 pages. <https://doi.org/XXXXXX.XXXXXXX>

1 INTRODUCTION

Face restoration, a domain-specific image restoration problem, is a classic task in the fields of image processing and computer vision. Face restoration is to restore the high-quality face image I_{hq} from the degraded face image $I_{lq} = \mathcal{D}(I_{hq}) + n_{\delta}$, where \mathcal{D} is the noise-irrelevant degradation function, and n_{δ} is the additive noise. According to different forms of the degradation function \mathcal{D} , the face restoration task can be divided into six main categories: (1)

Authors' addresses: Tao Wang, taowangzj@gmail.com, Nanjing University, Nanjing, China; Kaihao Zhang, Harbin Institute of Technology (Shenzhen), Shenzhen, China, super.khzhang@gmail.com; Jiankang Deng, Imperial College London, London, UK, j.deng16@imperial.ac.uk; Tong Lu, lutong@nju.edu.cn, Nanjing University, Nanjing, China; Wei Liu, Tencent, Shenzhen, China, wl2223@columbia.edu; Stefanos Zafeiriou, Imperial College London, London, UK, s.zafeiriou@imperial.ac.uk.

Permission to make digital or hard copies of all or part of this work for personal or classroom use is granted without fee provided that copies are not made or distributed for profit or commercial advantage and that copies bear this notice and the full citation on the first page. Copyrights for components of this work owned by others than ACM must be honored. Abstracting with credit is permitted. To copy otherwise, or republish, to post on servers or to redistribute to lists, requires prior specific permission and/or a fee. Request permissions from permissions@acm.org.

© 2025 ACM.

Manuscript submitted to ACM



Fig. 1. Examples of low-quality face images degraded from a high-quality (HQ) image, with respect to noise, blur, artifact, low resolution, and a mix of the above factors.

face denoising, which refers to removing the noise (e.g., Gaussian noise) contained in the face image [2, 89], (2) **face deblurring**, which is to recover a latent sharp face image from a blurry face image caused by various factors such as camera shake or object motion [110, 154], (3) **face super-resolution** (also known as face hallucination [170, 171]), which aims to enhance quality and resolution of low-resolution facial images [3, 180], (4) **face artifact removal**, which refers to recovering high-quality face images from the given low-quality face images with artifacts caused by lossy compression in the process of image storage and transmission [149, 175], (5) **blind face restoration**, which aims at restoring high-quality face images from the low-quality ones without the knowledge of degradation types or parameters [135, 149]. Fig. 1 illustrates exemplar low-quality face images caused by these forms of degradation, which influence not only the visual quality, but also the performance of down-stream computer vision algorithms. Thus, face restoration has a wide range of applications, including face recognition [68], privacy protection [159], and autonomous driving [14].

Early face restoration methods mainly focus on statistic prior and degradation models, which can be approximately divided into Bayesian inference based methods [3, 119], subspace learning based methods [35, 74], sparse representation based methods [121, 132], etc. In recent years, deep learning-based methods have attracted more and more attention with the development of deep learning and the availability of large-scale datasets. Thus, a large number of deep learning-based methods for face restoration have been proposed in the literature. Generally speaking, deep learning-based face restoration methods adopt different techniques to build state-of-the-art networks. The employed techniques mainly focus on the following aspects: different deep learning architectures [141, 142, 162, 164, 180], different facial priors [17, 32, 72, 161], different loss functions [17, 50, 71, 131], different learning strategies [70, 91], etc. Although deep learning solutions have dominated the research of face restoration in recent years, there is still a lack of in-depth and comprehensive surveys on face restoration with deep learning technology. Thus, this paper provides a comprehensive and systematic review of deep learning methods for the face restoration task.

Differences from Other Related Reviews. So far, there are few surveys about the overview of the face restoration task, though some surveys are related to the topic of face restoration. We divide them into three groups and discuss their differences in the following. (1) The first group [116, 120, 139, 151, 173, 173] aims to discuss general image restoration using deep learning techniques. For example, in [120, 139, 146, 151, 173], they discuss the common causes of one specific task in image restoration, such as deraining, denoising, super-resolution, and deblurring, respectively, and review different deep learning-based methods. [116] pays more attention to reviewing deep learning methods for general image restoration tasks that include image deblurring, denoising, dehazing, and super-resolution. (2) The second group [76, 98, 102, 133] focuses on reviewing the advances and development in traditional face super-resolution methods such as subspace learning based methods [35, 74], and sparse representation based methods [121, 132]. (3) The third group [48, 79] reviews the recent development in face super-resolution with deep learning techniques. Although the topic is related to ours, they focus only on the specific task of face super-resolution, whose scope is narrower

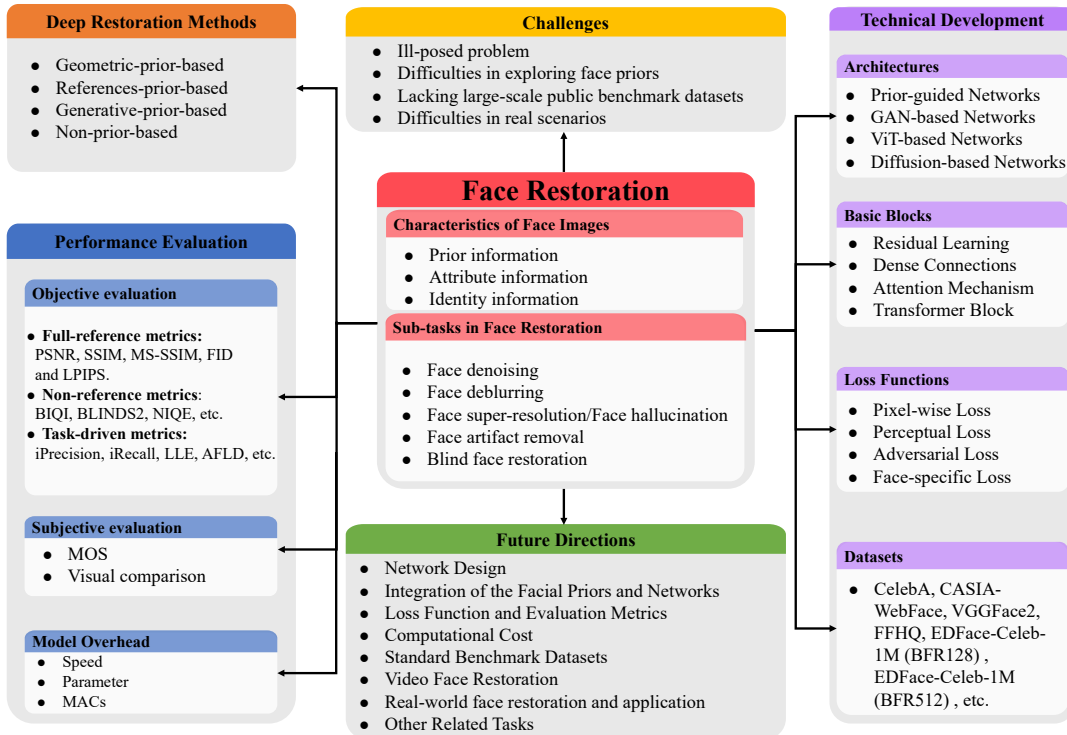


Fig. 2. Taxonomy of this survey on face restoration using deep learning techniques.

than ours. Differently, our work systematically and comprehensively reviews recent advances in deep learning-based methods for face denoising, face deblurring, face super-resolution, face artifact removal, and blind face restoration.

Our Contributions. This work systematically and comprehensively reviews the research progress of face restoration technology in recent years. The taxonomy of this survey is shown in Fig. 2. We conduct this survey in different aspects, including problem formulation, existing challenges, state-of-the-art methods, technical development, performance evaluation, and future directions. The contributions of this paper are summarized as follows. (I) We discuss the main degradation models in face restoration, the commonly used metrics, and the characteristics of face images that differ from natural images. (II) We discuss existing challenges in face restoration and provide a comprehensive overview of existing deep learning-based face restoration methods. (III) We provide in-depth analysis and discussion about the technical development of the methods, covering network architectures, basic blocks, loss functions, and benchmark datasets. (IV) We conduct a benchmark study of representative methods on popular face benchmarks, which will facilitate future experimental comparisons. (V) We analyze the open challenges of the face restoration task and discuss its future directions to guide future research for the community.

Organization of This Review. The remainder of this paper is organized as follows. In Section 2, we successively introduce the problem definitions of six common face restoration tasks, the image quality evaluation metrics, and the characteristics of face images. In Section 3, we discuss the challenges of face restoration and analyze how existing face restoration methods address these challenges. Section 4 reviews the technical development of deep face restoration,

including network architectures, basic blocks, loss functions, and datasets. Section 5 reports the experimental results of existing methods. In Section 6, we discuss the future directions of face restoration. Finally, Section 7 concludes this paper.

2 BACKGROUND

Problem Formulation. Image degradation during formation, transmission, and storage can take various forms in real-world facial images, including additive noise, spatially invariant or variant blur, aliasing, and compression artifacts. Generally, the degradation model is formulated as:

$$I_{lq} = \mathcal{D}(I_{hq}; n_\delta), \quad (1)$$

where I_{lq} is the low-quality face image, \mathcal{D} refers to the degradation function, I_{hq} is the corresponding high-quality face image, and n_δ usually denotes additive white Gaussian noise with a noise level δ . By specifying different \mathcal{D} , one can get different degradation. For example, noise degradation [1, 167] that \mathcal{D} is an identity function. Blur degradation [60, 173] where \mathcal{D} is a convolution/averaging operation. Low-resolution degradation [24, 24, 77, 136, 152] when \mathcal{D} is a combination of the convolution and downsampling operations. Artifact degradation [23, 81] when \mathcal{D} is a JPEG compression operation. Mixed degradation [135, 149] when \mathcal{D} is a combo of various factors.

FR refers to the recovery of a high-quality face image from its degraded low-quality counterpart. Namely, it aims to find the inverse of the degradation model in Eq. 1 as:

$$I_{hq} = \mathcal{D}^{-1}(I_{lq}; n_\delta), \quad (2)$$

where \mathcal{D}^{-1} is the face restoration model. If the degradation factors are provided, the FR task is regarded as non-blind face restoration, like face denoising, face deblurring, face super-resolution, and face artifact removal. Otherwise, the FR task is called blind face restoration. In the following, we detail the specific problem definition of sub-tasks in FR, where we mainly introduce some commonly used degradation models.

Face Denoising. This sub-task focuses on removing noise from an observed noisy face image. The noisy face image is typically constructed by the additive model, which is formulated as:

$$I_n = I_c + n_\delta, \quad (3)$$

where I_c , I_n , and n_δ represent the clean face image, noisy face image, and additive Gaussian noise with a noise level δ , respectively. Face Denoising is to find the inverse of the degradation model.

Face Deblurring. Face blur is a common problem in captured face images. It mainly contains motion blur [172] caused by the relative movement between the object and the camera, out-of-focus blur [16] caused by the misalignment between the target and the camera focus. Face deblurring mainly considers motion blur, which can be modeled as:

$$I_b = k_\sigma * I_s + n_\delta, \quad (4)$$

where I_b is the blurry face image, I_s is the sharp face image, k_σ is the blur kernel, $*$ is the convolution operation, and n_δ is the additive noise. Face deblurring is to obtain the inverse function of the degradation model, so as to generate sharp face images.

Face Super-resolution. As a domain-specific image super-resolution problem, face super-resolution refers to enhancing the resolution of low-resolution (LR) face images and producing high-resolution (HR) face images with rich details. The

degradation model is formulated as:

$$I_{lr} = (I_{hr} * k_{\sigma}) \downarrow_s + n_{\delta}, \quad (5)$$

where I_{lr} is the low-resolution face image, I_{hr} is the high-resolution face image, k_{σ} is the blur kernel, $*$ is the convolutional operation, n_{δ} is the noise, and \downarrow_s is the downsampling operation with a scale factor s . s is usually set as 2, 3, 4, and 8 in the face super-resolution task. Based on the degradation, face super-resolution aims to simulate the inverse process of the degradation model and recover the HR face image from the LR face image.

Face Artifact Removal. In real-world applications, lossy compression techniques (e.g., JPEG, Webp, and HEVC-MSP) are widely adopted for saving storage space and bandwidth. However, lossy compression easily leads to information loss and introduces undesired artifacts for recorded face images. Given a high-quality face image I_{hq} , its compression process is as follows:

$$I_{lq} = J(I_{hq}) + n_{\delta}, \quad (6)$$

where I_{lq} is the compressed face image, J denotes the image compression. As JPEG is the most extensively used way for image compression, researchers thus focus more on this type of degradation in the task of face artifact removal. According to the image compression process, face artifact removal is devoted to learning the inverse process of the degradation model and generating HQ face images.

Blind Face Restoration. Unlike focusing on a single type of degradation, blind face restoration aims to handle severely degraded face images in the wild. The degradation of face images is complex in this task, which is a random combination of noise, blur, low resolution, and JPEG compression artifacts. The degradation model of blind face restoration can be defined as:

$$I_{lq} = \{JPEG_q((I_{hq} * k_{\sigma}) \downarrow_s + n_{\delta})\} \uparrow_s, \quad (7)$$

where $*$ is the convolution operation, k_{σ} is the blur kernel, $JPEG_q$ is JPEG compression function with quality factor q , \downarrow_s is downsampling operation with scaling factor s , n_{δ} is the noise, and \uparrow_s is upsampling operation with scaling factor s . The goal of blind face restoration is to recover HQ face images by modeling the inverse process of the above degradation model.

Image Quality Assessment. Evaluating the quality of restored images is essential. Image quality assessment methods are generally categorized into subjective and objective approaches. Subjective evaluation, such as the Mean Opinion Score (MOS) [39], involves human raters assigning visual scores. While accurate, this method is costly and time-consuming. Objective evaluation is more practical and can be divided into full-reference, no-reference, and task-driven metrics. *Full-reference metrics* compare the restored image with its ground truth. Common metrics include PSNR [38], SSIM [138], MS-SSIM [140], and LPIPS [176]. PSNR measures pixel-wise differences, while SSIM also considers luminance, contrast, and structure. MS-SSIM enhances SSIM by aggregating local similarities. Unlike these pixel-based metrics that often favor overly smooth results, LPIPS evaluates perceptual similarity aligned with human vision. *No-reference metrics* estimate quality without ground truth. Widely used ones in face restoration (FR) include BIQI [95], BLINDS2 [104], BRISQUE [92], CORNIA [155], DIIIVINE [96], SSEQ [82], NIQE [93], and FID [36]. Among them, NIQE and FID [135, 141, 175] are commonly adopted to assess the naturalness of restored faces. *Task-driven metrics*, specific to face restoration, consider identity-related features. Examples include iPrecision, iRecall [179], LLE [149], Deg [135], AFLD, and AFICS [175], which evaluate fidelity using landmarks, face IDs, or identity similarity.

Analysis of Face Image. As we can see, the captured face images contain a wide variety of information related to humans, such as human face geometry spatial distribution information. Thus, different from the general image restoration task, the face geometry information (*i.e.*, facial prior) can be exploited for face restoration. In the past



Fig. 3. Left: Illustration of typical attributes in face images. Right: Examples of common face priors. The top row shows face images, while the bottom row presents the corresponding priors, including facial landmarks [17, 55], facial heatmaps [161], facial parsing maps [13], facial dictionaries [70], and 3D face priors [42].

decades, a large amount of human face information in face images has been explored to assist in face restoration. Generally speaking, the information in the face image can be divided into three categories: human attribute information, human identity information, and other prior information. We introduce them as follows.

Human Attribute Information. As illustrated in Fig. 3, a face image usually contains special attributes of a figure, such as gender, age, glasses, emotion *etc.* These face affiliated attributes are beneficial to multiple tasks, including face recognition [20, 124], face verification [59], and face restoration [80, 145]. As the degradation in face images is rather diverse and complex, it is difficult for the restoration model to recover the clear image relying only on the degraded image. Therefore, some methods [22, 80, 135] exploit human attributes in the face image as additional information to guide the restoration process. For example, Liu *et al.* [80] introduce the class-attribute information into the local detail restoration stage to further enhance local details.

Human Identity Information. In addition to the basic attributes in the face image, each face has its unique identity information. The identity information can be used to guide the model to generate faces close to the real identity. On the one hand, humans' accurate perception of the face mainly depends on the identity information of the face. On the other hand, adopting only the pixel-level loss to supervise the restoration model training cannot produce accurate identity-related facial details for the task of face restoration. For example, [91] can generate face images with high perceptual quality. However, it can not retain the face identity well in the recovered images. Thus, the identity information is introduced to improve both the recognizability and performance of face restoration in the literature [15, 31, 174].

Other Prior Information. As illustrated in Fig. 3, some representative facial priors in face restoration are facial landmarks [17, 55], facial heatmaps [161], facial parsing maps [13], and 3D face prior [42]. 1) Facial landmarks. There are some important reference points of facial components, such as eye centers, nose tips, and mouth corners of humans in the image. Different datasets provide different numbers of facial landmarks for each face image. For instance, CelebA dataset contains 5 landmarks [86], FFHQ dataset includes 68 landmarks [53], and Helen dataset provides 194 landmarks [62]. In addition, various facial landmark detection methods [25, 144] can help detect landmarks. 2) Facial heatmaps. Compared to facial landmarks directly providing reference points of facial components, facial heatmaps describe the probability that reference points are facial landmarks. Specifically, based on the facial landmarks, each landmark is encoded by using a 2D Gaussian centered at the coordinates of that landmark to generate the facial heatmaps. 3) Facial parsing maps. These are semantic feature maps of face images, which are separated out face components (*e.g.*, nose, skin, eyes, and hair) from the face images. 4) 3D face prior. In contrast to the 2D prior without considering high-dimensional

information (e.g., position and shape of faces), the 3D face prior is developed for face restoration [42]. 3D face prior provides rich 3D knowledge based on the fusion of different face attributes (e.g., identity, facial expression, illumination, and face pose). In addition, reference-based prior [70, 72] and generative prior [32, 135] are introduced in the literature to guide the face restoration models.

3 LITERATURE SURVEY

In this section, we first briefly analyze the challenges in face restoration tasks. Then, we present a systematic overview of face image restoration methods, including prior based deep restoration methods and non-prior based deep restoration methods.

3.1 Face Restoration Challenges

As a domain-specific image restoration task, face restoration aims to remove various unknown degradations in the low-quality face image and construct a high-quality one. However, there are several challenges in the task of face restoration.

Ill-posed problem. Although most existing methods are specifically developed for dealing with a single face restoration task, it is still an ill-posed problem, as the degradation types and degradation parameters of low-quality face images are unknown in advance. On the other hand, in practical scenarios, the degradation of face images is complex and diverse. Thus, designing effective and robust face restoration models to restore clear face images is a challenging problem.

Difficulties in exploring face priors. As a domain-specific image restoration task, some facial priors can be explored for face image restoration. Typical facial priors used in the literature include 1D vectors (identity and attributes), 2D images (facial landmarks, facial heatmaps, and facial parsing maps), and 3D prior. However, it is difficult to exploit the prior knowledge, because facial priors such as facial components and facial landmarks are usually extracted or estimated from low-quality images, which may be inaccurate and therefore directly affect the restoration performance. On the other hand, real-world low-quality images often contain complex and diverse degradation, and it is difficult to find appropriate priors to assist the process of face restoration. In addition, face restoration is different from image restoration due to the specialty of face images. For example, human eyes are more sensitive to face artifacts, bearing in mind a strong expectation of human face structure. Thus, it brings another difficulty in restoring the human face.

Lacking large-scale public benchmark datasets. With the development of deep learning techniques, deep learning-based methods have shown impressive performance in face restoration. Most deep learning-based face restoration methods strongly rely on large-scale datasets to train networks. However, most of the current face restoration methods are trained or tested on non-public datasets. Especially in their experiments, these methods usually synthesize low-quality images using their private schemes based on the high-quality images and randomly split them for training and evaluation respectively [8, 131, 180]. Though some works use fixed training/testing sets [32, 70, 135, 149], the synthesized low-quality images are still different due to random noise, random combinations of degradation factors, etc. Therefore, it is still difficult to directly compare existing methods based on the reported results. Lacking public datasets directly leads to unfair performance comparison. In addition, lacking high-quality and large-scale benchmarks limits the potential of models. Therefore, it is a challenge to build more proper benchmark datasets for face restoration.

Difficulties in real-world scenarios. Though deep learning methods have acquired state-of-the-art performance in face restoration, most of them work in a supervised manner. Specifically, these approaches require a paired (low-quality and high-quality image pair) dataset, and they would fail if the conditions are unsatisfied. However, it is difficult to collect

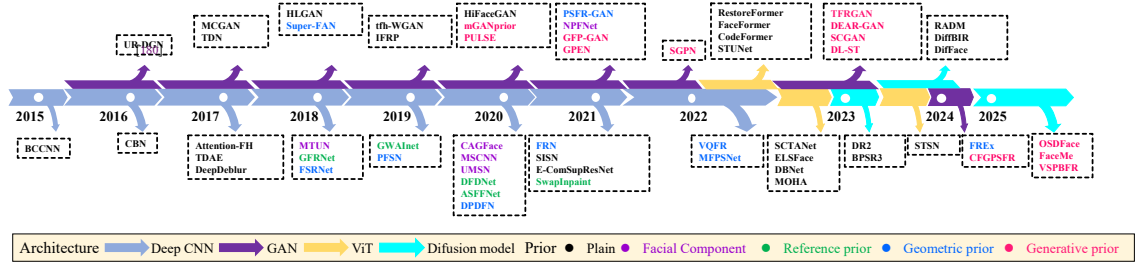


Fig. 4. Milestones of deep learning-based face restoration methods. We summarize the methods by different network architectures and facial priors. We list their names in the figure.

large-scale datasets with real paired samples in the real world due to the complex and changeable scene. Therefore, most methods synthesize low-quality images by degradation models to approximate the real low-quality image. In addition, the synthesized low-quality face images are probably less informative and inconsistent with real-world images. The models trained on synthetic data sets can easily lead to domain drift, which limits the applicability of the model in real scenarios.

In the following, we will introduce and analyze in detail how existing face restoration methods deal with the above challenges.

3.2 Face Restoration Methods

General image restoration methods aim to design efficient methods for recovering sharp natural images. However, as a highly structured object, the human face has specific characteristics that are ignored by general image restoration methods. Thus, most face restoration methods incorporate face prior knowledge to recover facial images with clearer facial structure. The developed face-specific priors in the models are mainly based on common sense that human faces exhibit small variations in a controlled environment. On the other hand, other methods aim to develop networks learning a mapping function between the low-quality and high-quality face images without the facial prior. The milestones of face restoration in the past years are illustrated in Fig. 4. We divide face restoration methods into two categories: prior based deep restoration methods and non-prior based deep learning approaches. In addition, prior based deep restoration methods can be approximately divided into three sets: geometric prior based deep restoration methods, reference prior based deep restoration methods, and generative prior based deep restoration methods. In the following, we discuss these methods in detail.

Geometric Prior Based Deep Restoration Methods. These methods mainly adopt the unique geometry and spatial distribution information of faces in the image to help the model progressively restore high-quality face images. Typical geometric priors include facial landmarks [17, 55], facial heatmaps [161] and facial parsing maps [13]. Chen *et al.* [17] make the first attempt to design a specific face geometric prior estimation sub-network in a deep network and train them in an end-to-end manner for the face super-resolution task. Specifically, they first use a coarse network to recover the coarse high-resolution image. Then the coarse image is sent to a fine super-resolution network and a prior information estimation network to extract image features and estimate landmark heatmaps and parsing maps respectively. In the end, both image features and geometric prior are fed to a fine super-resolution decoder to restore high-resolution images. This pioneering work improves the performance of face super-resolution while also providing a

solution to estimating geometric prior directly from low-quality face images. Another representative work is Super-FAN proposed by Bulat and Tzimiropoulos [6]. Super-FAN is the first end-to-end system to simultaneously achieve facial super-resolution and facial landmark localization. The core insight in Super-FAN is using the joint training strategy to guide the network to learn more face geometric information, which is achieved by integrating a face-alignment sub-network via heatmap regression and loss optimization. To further utilize facial attributes around the landmark for restoring facial details, Kim *et al.* [55] propose a lightweight face alignment network to generate facial landmark heatmaps for the face super-resolution network by a progressive training method. For example, by including the parsing map, an additional face prior is provided, which improves the network's performance in repairing the faces. Recently, Chen *et al.* [13] propose a multi-scale progressive model for face restoration, which recovers low-quality face images in a coarse-to-fine manner by semantic-aware style transformation.

Compared with accurately estimating face landmarks or semantic maps directly from low-quality images, it is easy to localize facial components (not landmarks). Thus, another line of geometric prior based methods [51, 56, 110, 154, 161] is to take advantage of features of the facial component in human faces, *e.g.*, eyes and nose, as the prior information. For example, MTUN [161] is one representative method that contains two branches. The first branch is used to super-resolve face images. The second branch is designed for estimating facial component heatmaps, where four heatmaps are employed to represent four components (*i.e.*, eyes, nose, mouth, and chin) of a human face. MTUN shows that utilizing information of facial components in low-quality face images can further improve the performance of face restoration. Recently, Yu *et al.* [165] make the first attempt to take full advantage of multi-geometric priors (*i.e.*, semantic-level parsing maps, geometric-level facial heatmaps, reference-level facial dictionaries, and pixel-level degraded image information) in the proposed network to guide face restoration. In contrast to the previously mentioned methods that focus on using 2D priors, Hu *et al.* [42] make the first attempt to embed 3D priors into networks for general face recovery tasks. Compared with 2D priors, 3D priors can integrate parameter descriptions of face attributes (*e.g.*, identity, facial expression, texture, illumination, and facial pose) to provide 3D morphological knowledge and further improve the face restoration performance.

Reference Prior Based Deep Restoration Methods. Previous works exploit facial prior purely relying on a single degraded image. It is worth noting that the degradation process is generally highly ill-posed, which fails to obtain an accurate facial prior. Thus, several methods aim to guide the face restoration process by using the facial structure or facial component dictionaries obtained from additional high-quality face images as reference prior [22, 70–72]. Some reference prior based methods utilize the additional information provided by a high-resolution guiding image with the same identity. Li *et al.* [72] and Dogan *et al.* [22] mainly employ a fixed frontal high-quality reference for each identity to provide additional identity-aware information to help the process of face restoration. Specifically, Li *et al.* propose a guided face restoration network (GFRNet) model consisting of a warping sub-network (WarpNet) and a reconstruction sub-network (RecNet) for face restoration. The WarpNet provides warped guidance, which aims to generate the flow field for warping the reference image to correct the pose and expression of the face. The RecNet takes both the low-quality image and warped guidance as input to recover the high-quality face image. In addition, due to the unavailability of the ground-truth flow field, they introduce a landmark loss to train WarpNet. Based on GFRNet, Dogan *et al.* [22] propose a GWAInet for face super-resolution, which is trained in an adversarial generative manner to generate high-quality face images. Compared with GFRNet, GWAInet does not rely on facial landmarks in the training stage, which guides the model to focus more on the whole face region and increases the robustness of the model. These two methods use a WarpNet to predict the flow field to warp the reference to align with the low-quality images. However, the alignment still does not fully solve all the differences between the reference and low-quality

images, *i.e.*, mouth close to open. Furthermore, these two methods rely on a high-quality reference image with the same identity, which makes them only applicable in limited scenes. Thus, Li *et al.* [70] propose a deep face dictionary network (DFDNet) for face restoration, which uses deep component dictionaries as the reference prior to benefit the restoration process. In DFDNet, Li *et al.* first adopt K-means to produce facial component dictionaries for perceptually significant face components (*i.e.*, left/right eyes, nose, and mouth) from high-quality images. Then, they choose the most similar component features from the generated component dictionaries to transfer the details to the low-quality face image and guide the model for face restoration. Recently, Li *et al.* [73] propose a DMDNet model, which explicitly memories the generic and specific features through dual facial dictionaries in the network for blind face restoration. To recover face well on mobile phones with limited memory and processing budget, Lai *et al.* [61] develop a face deblurring system based on the dual camera fusion technique for mobile phones, which can promote the further development of reference-based face deblurring.

Generative Prior Based Deep Restoration Methods. With the rapid development of generative adversarial network (GAN) [53, 54], recent works find that [32, 91] the generative prior of pre-trained face GAN models, such as StyleGAN [53] and StyleGAN2 [54], can provide rich and diverse facial information (*e.g.*, geometry and facial textures). And researchers have started to leverage the GAN prior to face image restoration. The first kind of generative prior based methods is inspired by GAN inversion methods, which mainly aim at finding the closest latent vector in the GAN span from the input image. PULSE [91] is another representative method, which is a self-supervised face restoration method by optimizing the latent of a pre-trained StyleGAN [53]. Inspired by PULSE, mGANprior [32] considers multiple latent codes in the pre-trained GAN and optimizes multiple codes to promote the ability of image reconstruction. However, these methods fail to preserve fidelity in the restored face images. To achieve a better balance between visual quality and fidelity of the recovered images, recent works GFP-GAN [135] and GPEN [150] first extract fidelity information from the input low-quality face images and then leverage the pre-trained GAN as a decoder to capture facial prior. Specifically, GFP-GAN [135] leverages the facial distribution captured by a pre-trained GAN as the facial prior in order to achieve joint restoration and color enhancement. GFP-GAN contains a degradation removal module and a pre-trained face GAN as facial prior. These two modules are bridged by latent code mapping and several channel-split spatial feature transform layers, which can achieve a good balance of realness and fidelity. GPEN [150] aims to effectively integrate the advantages of GAN and DNN for face restoration. In GPEN, it first learns a GAN used for generating high-quality face images and embeds this pre-trained GAN into a deep neural network as a decoder prior for face restoration. More recently, Zhu *et al.* [182] propose to combine shape and generative prior to guide the process of face restoration for the network. In the proposed network, they first use a shape restoration module to generate a shape prior. Then, a shape and generative prior integration module is proposed to fuse the shape and generative prior. Finally, they introduce a hybrid-level loss to jointly optimize the shape and generative prior with other network parts, and thus, these two priors can better benefit the face restoration. To address severe degradation in facial images, Xie *et al.* [147] introduce a novel framework named TFRGAN. This framework focuses on generating a more accurate and improved latent code for the StyleGAN2 prior by incorporating both text and image information within the latent code space. In addition to utilizing generative priors, recent methods [11, 40, 43] also propose novel frameworks to leverage the representation of degradation and generative priors in face images. These methods aim to achieve a balance between realism and fidelity when dealing with diverse levels of degradation.

Non-prior Based Deep Restoration Methods. Although most deep learning-based FR methods can recover satisfying faces with the help of the facial prior, it makes the cost of generating face images expensive and laborious. To address this problem, many methods aim to design a network that directly learns the mapping function between

low-quality and high-quality face images without any additional facial priors. Some techniques are introduced in the models to improve the feature representation, such as multi-path structure, attention mechanism, feature fusion strategy, adversarial learning, strong backbone *etc.*

The first representative work is dated back to 2015. Zhou *et al.* [180] propose a bi-channel convolutional neural network (BCCNN) for face super-resolution. It consists of a feature extractor and an image generator. The proposed feature extractor extracts robust face representations from the low-resolution face image. The image generator is designed to adaptively fuse the extracted face representations and the input face image to generate a high-resolution image. BCCNN can achieve better restoration results for the face image with large variations. However, this work directly ignores pre-aligned facial spatial configurations (such as facial landmark localization) and thus does not perform well when the input image has severe blur. To address this problem, Zhu *et al.* [184] propose a cascade bi-network called CBN to jointly optimize facial dense correspondence field estimation and face super-resolution. CBN obtains better performance results than previous works. However, when the face feature location in the model is wrong, CBN may generate ghosting face images.

Following previous works [180, 184], some state-of-the-art methods [8, 49, 129, 131, 164] focus on designing different CNN networks and learning strategies, such as partial [78] and Fourier [117] convolution, recurrent learning strategy [65], and multi-path structure [49], to improve the performance of the network. Among them, [49] is a representative work that aims at using recurrent and multi-path structures in the network to improve performance. Jiang *et al.* [49] propose a dual-path deep fusion network (DPDFN) for face super-resolution. The core insight of DPDFN is local and global feature learning and fusion in two branches. A convolutional denoising autoencoder network is proposed in [125] for face denoising, which can achieve superior denoising performance by leveraging robust spatial correlations. Over the past few years, GAN [30] has become another popular technology in the computer vision community. It has been widely applied in many applications, including image synthesis, semantic image editing, style transfer, classification, and image restoration. Compared with CNN, GAN can generate more realistic images [19]. The typical GAN structure consists of a generator network and a discriminator network. The generator is designed to produce realistic images, and the discriminator is used to figure out the difference between the image produced by the generator and the real image. The generator and discriminator are trained at the same time and compete against each other. In 2016, Yu and Porikli [162] make the first attempt to develop GAN and propose ultra-resolution by discriminative generative networks (UR-DGN) for face restoration. In UR-DGN, through an adversarial learning strategy, the discriminant network is used to learn the important components of human faces, and the generation network fuses these facial components into the input image. Following Yu and Porikli [162], many GAN based face restoration methods are proposed in the literature [7, 108, 112, 148, 149, 163]. These methods integrate many techniques (e.g., loss functions, learning strategies, identity constraints *etc.*) into the GAN network and achieve better visual results. Specifically, MCGAN [148] uses a multi-class GAN model and a feature matching loss. TDN [163] aims to exploit the class specific information in the process of restoration. HLGAN [7], th-WGAN [108], and HiFaceGAN [149] focus on designing more complex GAN models, including two-stage GANs, WGAN, and multi-stage GAN network. IFRP [112] adopts identity-preserving algorithms to help the GAN model produce high-quality face images with accurate identity information.

Since 2014, the attention mechanism has been gradually applied to visual tasks and has achieved great effects [41, 94]. The core idea of the attention mechanism is to reweight features through a learnable weight map to emphasize the important features and suppress the less useful ones. Many face restoration methods [12, 87, 137, 177] resort to the attention mechanism to improve their performance. Among them, [12, 137, 177] mainly design large-scale residual blocks with the attention mechanism to extract fine-grained face features, which can produce better performance.

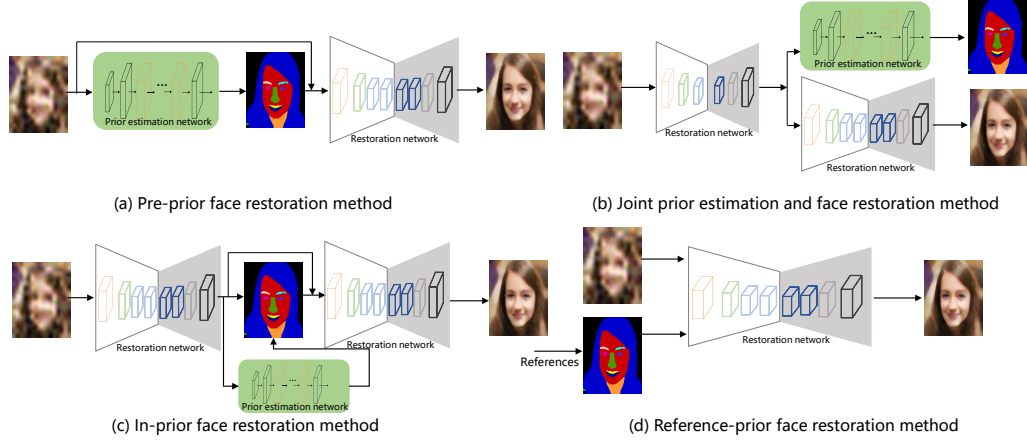


Fig. 5. Summary of the network architecture of prior-guided methods. It mainly consists of Pre-prior face restoration methods, Joint prior estimation and face restoration methods, In-prior face restoration methods, and Reference-prior face restoration methods. We use the facial parsing map as an example of prior in the figure.

However, they do not consider cross-channel interaction in the residual blocks, which reduces the ability of feature representation in the network. Thus, Lu *et al.* [87] propose a split-attention in the split-attention network (SISN) for face super-resolution. SISN is stacked by several external-internal split attention group (ESAG) modules. ESAG uses multi-path learning, attention mechanism, and residual learning to enable the network to focus on facial texture details and structure information simultaneously. With this specific module, SISN can generate high-quality faces containing more facial structural information. In addition, some recent works [122, 123, 158, 169] also design different attention mechanisms in the network to enhance the visual quality of the generated face images. For example, [169] proposes a self-attention learning network that utilizes a complementary three-stage face super-resolution architecture and a simple self-attention module to enhance the degraded input face. In [122, 123], the authors use spatial attention to help the network focus on preserving the facial structure features. In recent years, the Vision Transformer (ViT) architecture has shown great potential in computer vision. Many methods [4, 28, 64, 111, 141, 143, 175, 181] aim to use strong Transformer backbone to build face restoration networks and have demonstrated superior performance. Among them, several studies [64, 141, 175, 181] directly resort to the Transformer to enhance the network's global representation ability, resulting in improved performance. However, relying solely on image-level self-attention might lead to the loss of local fine-grained details. Therefore, some studies [4, 69, 100, 111, 143] aim to combine the strengths of convolutional neural networks (CNN) and Transformers to effectively utilize both global information and local features, thereby achieving high-quality face reconstruction. For example, Bao *et al.* [4] propose a spatial attention-guided CNN-Transformer aggregation network (SCTANet) for FSR. The core components are the hybrid attention aggregation block and the sub-pixel MLP-based upsampling module. In [100], [111] and [143], the authors also propose FSR frameworks incorporating Transformer and CNN architectures known as ELSFace, DBNet, and MOHA, respectively. Very recently, diffusion models, such as the diffusion denoising diffusion probability models (DDPM) [37] and the denoising diffusion implicit models (DDIM) [115], have garnered considerable attention in the task of face restoration [26, 29, 97, 101, 142, 166, 178]. When compared to other models, diffusion models exhibit greater capability in representing image pixel distribution. This characteristic presents substantial potential for enhancing visual quality and benefiting high-quality face restoration.

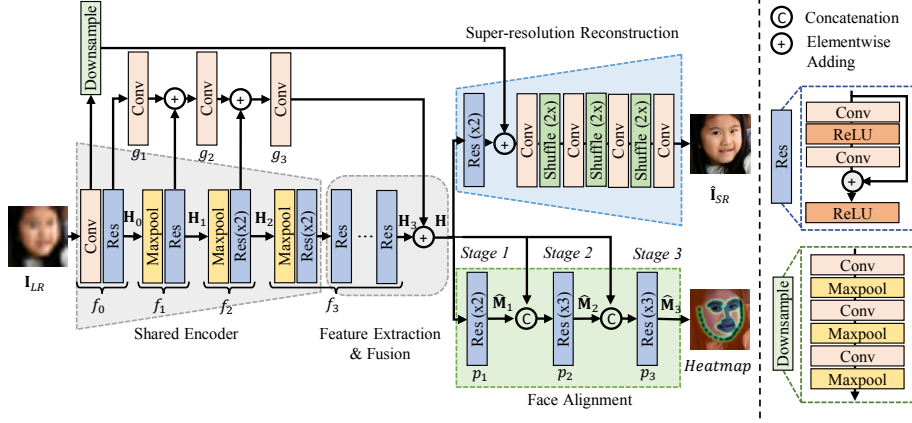


Fig. 6. Architecture to jointly learn landmark localization and face restoration in [157].

For example, Wang *et al.* [142] propose a diffusion-based robust degradation remover called DR2 for face restoration. DR2 involves initially transforming the degraded image into a coarse, degradation-invariant prediction. Subsequently, an enhancement module is employed to restore the coarse prediction and generate a high-quality face image. Gao *et al.* [29] propose a novel conditional generative model called BPSR3 for face super-resolution, which is based on diffusion models. Specifically, BPSR3 replaces the original U-Net, which is used in super-resolution via repeated refinement (SR3), with a multi-scale deep back-projection network structure.

4 TECHNICAL DEVELOPMENT REVIEW

In this section, we discuss the developments of existing face restoration in the following aspects: network architectures, basic blocks, loss functions, and benchmark datasets.

4.1 Network Architectures

Existing state-of-the-art networks are designed by focusing on facial prior, pre-trained GAN models, ViT architectures, and diffusion models. Thus, we discuss these developments in this section.

Prior-guided Networks. As a domain-specific image restoration task, it is important to consider the characteristics of face images (e.g., identity, structure, and face pose) when designing the specialized networks for face restoration. To this end, some priors are introduced into the networks to help the process of restoration. With the help of facial priors, these networks can generate realistic faces with details. According to the way of using priors, the architectures of the prior-guided networks can be divided into four categories: Pre-prior face restoration method, Joint prior estimation and face restoration method, In-prior face restoration method, and Reference-prior face restoration method. The summary of these architectures is illustrated in Fig. 5.

For pre-prior face restoration methods [13, 51, 109, 110], they usually adopt a prior estimation network (e.g., face passing network or a pre-trained face GAN) to extract prior from the low-quality input. For example, [109] designs a face parsing network to extract the semantic label from the input image or coarse deblurred image. Then it concatenates the input blurred image and the face semantic label to the deblurring network to generate the sharp image.

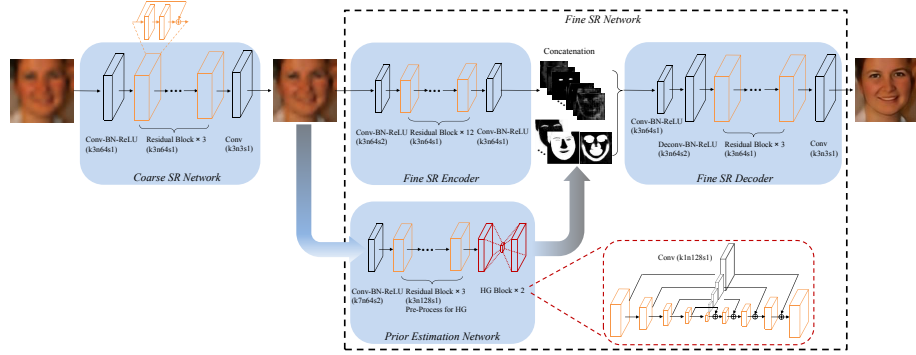


Fig. 7. Architecture to estimate face passing map in the middle of the network in [17].

The second type of method is the joint prior estimation and face restoration method, which takes advantage of the relationship between the prior estimation task and the face restoration task. These methods [66, 67, 157, 184] usually jointly train the face restoration network and the prior estimation network. This kind of method enjoys the benefit of two sub-tasks and directly promotes face restoration performance. For example, as illustrated in Fig. 6, Yin *et al.* [157] propose a joint alignment and face super-resolution network to jointly estimate facial landmarks and super-resolve face images.

However, directly extracting the face prior from low-quality images is difficult. Thus, in-prior face restoration methods [17, 90, 110, 161] first use a restoration network to produce the coarse recovered image, then extract the prior information from the coarse image, which can obtain a more accurate prior. FSRNet [17] is one representative method, which is shown in Fig. 7. In FSRNet, a coarse SR network is used to recover the coarse image, and then the coarse image with high quality is processed by a fine SR encoder and a prior estimation network respectively. After that, both image features and prior information are fed to the fine SR decoder to recover the final results.

In contrast to the above methods that estimate face priors directly or indirectly from low-quality images, reference-prior face restoration methods aim to exploit the high-quality images of the same person to alleviate the difficulty of facial prior estimation or image restoration. Some methods [22, 72] propose a warping subnet to align the reference and degraded images. Typical works are GFRNet [72] and GWANet [22]. In GFRNet [72], a landmark loss and a total variation regularization are designed to train the warping subnet. GWANet [22] trains the warping subnet in an end-to-end manner without the facial landmark and proposes a feature fusion chain with multiple convolution layers to fuse features from the warped guidance and degraded image. Recent works [70, 71] propose to exploit deep facial component dictionaries or use multiple high-quality exemplars in the face restoration to exploit more guidance features and thus improve the generalization ability when dealing with low-quality face images with unknown degradation.

GAN-based Networks. With the success of the GAN architecture, some works aim at designing specialized GAN networks for face restoration. As shown in Fig. 8, the architectures of GAN-based networks can be summarized as the plain GAN architecture and the pre-trained embedding architecture. In the plain GAN architecture-based methods [7, 148, 149, 162, 163], they introduce an adversarial loss in the network and use adversarial learning to jointly optimize the discriminator and generator (*i.e.*, face restoration network) to generate realistic face images. Among them, HLGAN [7] is one representative method for face super-resolution. HLGAN consists of two generative adversarial networks. The first network is a High-to-Low GAN, which is trained with unpaired images to learn the degradation

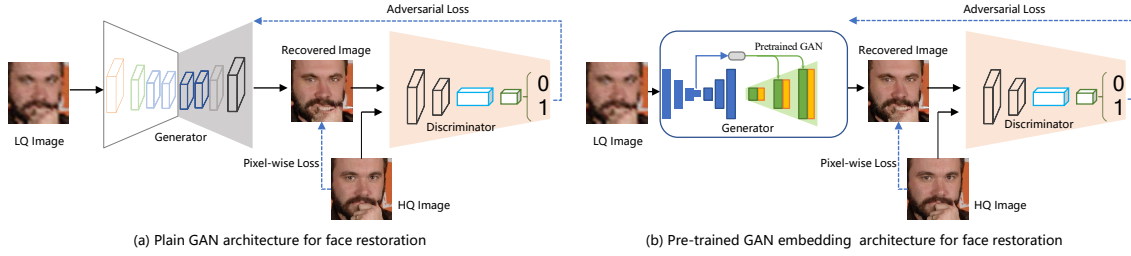


Fig. 8. Summary of GAN architecture used for face restoration. It mainly contains a plain GAN architecture and a pre-trained GAN embedding architecture.

process of the high-resolution images. After that, its outputs (*i.e.*, low-resolution face images) are adopted to train a Low-to-High GAN for face super-resolution. The second Low-to-High GAN is trained with paired face images. Thanks to this two-stage GAN architecture, HLGAN can achieve superior performance when dealing with real face images.

In pre-trained GAN embedding architecture-based methods [32, 91, 135, 150, 182], they exploit the latent prior in pre-trained face GAN models such as StyleGAN [53] and incorporate the prior into the process of face restoration. One representative work is GFP-GAN, which effectively leverages face priors encapsulated in the pre-trained face GAN to perform face restoration. The detail architecture of GFP-GAN [135] is illustrated in Fig. 9. Specifically, GFP-GAN is composed of a degradation removal module and a pre-trained face GAN. These modules are connected together by the latent code mapping and some channel-split spatial feature transform layers. In addition, a loss function combined with the pixel-wise loss, the facial component loss, the adversarial loss, and the identity preserving loss is proposed to train the GFP-GAN. With these techniques, GFP-GAN can recover high-quality face images with facial details.

ViT-based Networks. In recent years, the Visual Transformer (ViT) [27] architecture has demonstrated superior performance in natural language processing and computer vision. ViT triggers the direct application of the Transformer architecture [126] in computer vision tasks, including object recognition, detection, and classification [10, 27, 134]. ViT architecture also begins to be applied to the face restoration task. Wang *et al.* [141] propose RestorFormer based on ViT architecture for face restoration. RestorFormer aims at modeling contextual information of the face image to help the process of face restoration. Specifically, Wang *et al.* propose a novel multi-head cross-attention layer, which explores spatial interactions between corrupted queries and high-quality key-value pairs. The high-quality key-value pairs are from a learned high-quality dictionary. With the help of advanced architecture and the high-quality dictionary prior, RestorFormer recovers results with more texture details and complete structures. Zhou *et al.* [181] treat face restoration as a code prediction task that aims at learning the discrete codebook prior in a small finite proxy space. They thus propose a Transformer-based prediction network (CodeFormer) to achieve code prediction for face restoration.

To effectively process diverse scale face images, Li *et al.* [64] propose a novel scale-aware blind face restoration framework FaceFormer. They transform facial feature restoration as a facial scale-aware transformation procedure and then employ hierarchical Transformer blocks in the network to extract robust facial features. The FaceFormer produces high-quality face images with faithful details. Inspired by the success of Swin Transformer [85] on high-level vision tasks, Zhang *et al.* [175] propose an end-to-end Swin Transformer U-Net (STUNet) for face restoration. In STUNet, the self-attention mechanism and the shifted windowing scheme are used to help the model focus on important features for effective face restoration. Besides, they build two larger-scale face restoration benchmark datasets to further advance the development of face restoration and model evaluation. Although the above ViT-based methods

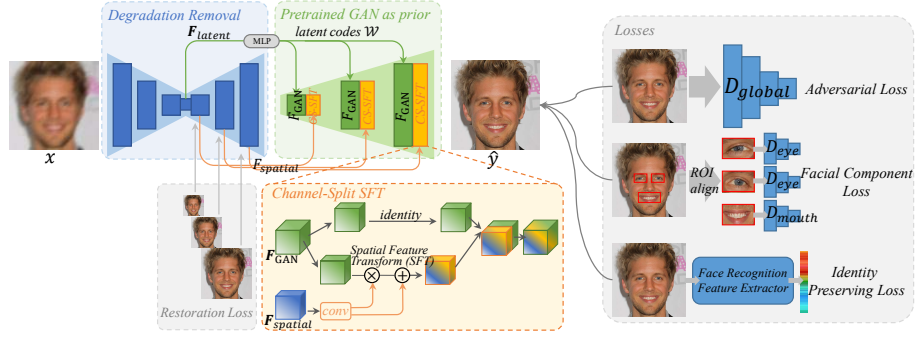


Fig. 9. The architecture of GFP-GAN [135], which is designed under the pre-trained GAN embedding architecture.

have demonstrated effectiveness in face restoration, there are still many problems to be studied, such as the model's efficiency and generalization in real-world scenery.

Diffusion Models based Networks. Recently, diffusion probabilistic models [37, 114, 115] have shown state-of-the-art performance in computer vision tasks. The core technique of diffusion probabilistic models is transforming the complex and unstable generation process into multiple independent and stable reverse processes through the use of Markov Chain modeling. In the task of face restoration, the denoising diffusion probabilistic model (DDPM) [37] is widely utilized. DDPN contains two key processes in the diffusion model, namely the forward process and the reverse process, which are briefly introduced as follows.

The forward process (*i.e.*, the diffusion process) is a fixed Markov Chain that sequentially corrupts an image $x_0 \sim p_{data}(x)$ at T diffusion time steps, by injecting Gaussian noise according to a variance schedule $\beta_1, \dots, \beta_T \in (0, 1)$. It can be formulated as:

$$q(x_t|x_{t-1}) = \mathcal{N}(x_t; \sqrt{1 - \beta_t} \cdot x_{t-1}, \beta_t \mathbf{I}). \quad (8)$$

Moreover, we can compute the probabilistic distribution of x_t given x_0 as:

$$q(x_t|x_0) = \mathcal{N}(x_t; \sqrt{\hat{\alpha}_t} x_0, \sqrt{1 - \hat{\alpha}_t} \mathbf{I}), \quad (9)$$

where $\alpha_t = 1 - \beta_t$ and $\hat{\alpha}_t = \prod_{i=1}^t \alpha_i$. Then, $x_T \sim \mathcal{N}(0, \mathbf{I})$ if T is larger enough.

The forward process aims to generate images in a progressive manner, which is achieved through a Gaussian transition with a learned mean μ_θ :

$$p_\theta(x_{t-1}|x_t) = \mathcal{N}(x_{t-1}; \mu_\theta(x_t, t), \tilde{\beta}_t \mathbf{I}), \quad (10)$$

where $\mu_\theta(x_t, t) = \frac{1}{\sqrt{\alpha_t}}(x_t - \frac{\beta_t}{\sqrt{1 - \hat{\alpha}_t}})\epsilon_\theta(x_t, t)$ for $\epsilon \sim \mathcal{N}(0, \mathbf{I})$ and $\tilde{\beta}_t = \frac{1 - \hat{\alpha}_{t-1}}{1 - \hat{\alpha}_t}$. The variance schedule β_t is predefined, and thus, it only requires approximating the mean $\mu_\theta(x_t, t)$ by a denoising network $\epsilon_\theta(x_t, t)$. Fig. 10 shows the forward and reverse processes of denoising diffusion probabilistic models.

Recent researchers utilize diffusing models for face restoration [83, 88, 130]. Different from existing diffusion-based methods (*e.g.*, SR3 [106]) that use U-Net as their backbone network, Gao *et al.* [29] replace the U-Net in super-resolution via repeated refinement (SR3) with a multi-scale deep back-projection network structure. This modified diffusion model obtains a faster convergence and better restoration quality for face images with fewer parameters than the original SR3. In [166], the authors introduce a diffusion-based method named DiffFace for face restoration. Notably, DiffFace utilizes a pre-trained restoration network, such as SRCNN [24] or SwinIR [75], to acquire an initial clean image that serves as the

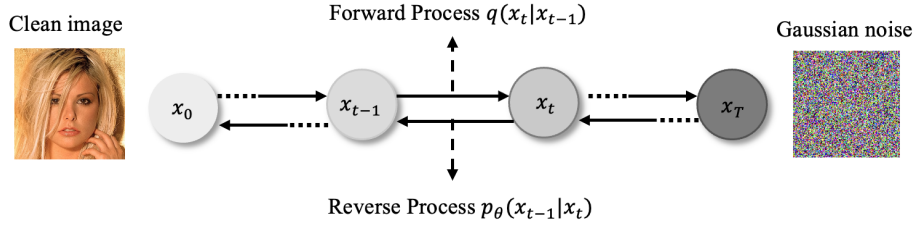


Fig. 10. Illustration of denoising diffusion probabilistic models.

starting point for the diffusion model's sampling process. This unique design enhances the generalization capability of the diffusion model in handling severe and unknown degradations in face images. In contrast, Wang *et al.* [142] propose a diffusion-based framework called DR2E for face restoration. Specifically, DR2E contains two stages. In the first stage, DR2 transforms the degraded images into coarse results that belong to a degradation-invariant distribution. In the second stage, the enhancement module further processes the degradation-invariant images to produce high-quality details.

4.2 Basic Blocks

In the field of face restoration, different types of basic blocks are designed to build powerful face restoration networks. In this section, we detail basic blocks that are widely used in the network.

Residual Learning and Dense Connections. Residual learning and dense connections are two widely adopted strategies in face restoration to enable deeper networks, mitigate gradient issues, and promote feature reuse.

Residual Learning. Introduced in ResNet by He *et al.* [34], residual blocks use skip connections to alleviate vanishing/exploding gradients and allow deeper architectures. Many face restoration methods [13, 17, 42, 55] adopt residual learning, which can be categorized into two types:

- Global Residual Learning (GRL) focuses on predicting the residual between the input and target images rather than generating the clean image directly [118]. Since most residual values are near zero, this simplifies learning and improves convergence [13, 149, 175].
- Local Residual Learning (LRL) applies residual connections within network modules. It is frequently used to stabilize training and enhance feature extraction [7, 131, 135]. For instance, Chen *et al.* [17] utilize residual blocks in FSRNet to construct coarse/fine SR networks and a prior estimation module. Some works combine GRL and LRL to leverage the benefits of both [18, 149, 175].

Dense Connections. Huang *et al.* [44] propose DenseNet, where each layer connects to all preceding layers. This architecture encourages feature reuse, strengthens gradient flow, and supports multi-level feature fusion. In face restoration, dense connections have proven effective [49, 84, 124]. For example, Tu *et al.* [124] apply dense links in the decoder to enhance spatial detail reconstruction. Jiang *et al.* [49] further integrate residual, dense, and recursive modules in DPDFN, forming a memory-driven sub-network that improves information flow and boosts performance.

Attention Mechanism. With the successes of the attention mechanism in various vision tasks, the attention mechanism has been widely employed in face restoration networks [8, 42, 55]. Among them, the utilized attention techniques can be divided into channel attention, spatial attention, hybrid attention, and other attention mechanisms.

Channel Attention. The channel attention is to learn the relative weights between feature channels and make the model focus on the important feature channels. For example, Chudasama *et al.* [18] propose an E-ComSupResNet network with channel attention to super-resolve low-resolution face images. In E-ComSupResNet, it integrates the channel attention into the Resblock to rescale the channel-wise feature maps adaptively.

Spatial Attention. The spatial attention focuses on capturing the spatial contextual information of the feature. For instance, Chen *et al.* [12] introduce a spatial attention mechanism to the residual blocks and use the modified block to build a network. With the guidance of spatial attention, the network can pay more attention to features related to the key face structures.

Hybrid Attention. Some methods use channel and spatial attention mechanisms to improve the representation of the network. For instance, to exploit the 3D face rendered priors in the network, Hu *et al.* [42] develop a spatial attention module (SAM) with channel and spatial mechanisms to capture the locations of face components and the facial identity. This module effectively exploits the hierarchical information of 3D faces to help the network generate high-quality face images.

Other Attention. Some methods do not use the attention mechanism in the network design. On the contrary, they aim to propose an attention-based loss to optimize the network. One representative work is PFSN [55], which uses facial heatmaps to produce a mask and obtains facial attention loss by computing the difference between the mask recovered and high-quality face images.

Transformer Block. Due to its strong capability to capture long-range dependencies between sequences, the recent Transformer has been a popular architecture in the computer vision community. The vision Transformer architecture usually decomposes an input image into a sequence of local windows and uses the self-attention mechanism to learn their relationships. We divide the Transformer block into the plain Transformer and the Swin Transformer.

Plain Transformer. The original Transformer block is proposed in [27]. It contains a normalization layer, a multi-head self-attention layer, and a feed-forward network layer. Recent methods [141, 181] employ the plain Transformer block to build network modeling global interrelations. For example, RestoreFormer [141] performs the cross-self-attention mechanism between corrupted queries (extracted from input image) and high-quality key-value (sampled from high-quality dictionary) pairs by Transformer blocks. With the help of Transformer blocks, RestoreFormer can recover a clear face with realness and fidelity.

Swin Transformer. To reduce the complexity of the plain Transformer, Liu *et al.* [85] propose the Swin Transformer layer to build an efficient Transformer network called Swin Transformer. The main difference between the Swin Transformer layer and the plain Transformer is that it adopts local attention and window shifting mechanisms to realize multi-head self-attention. Due to its impressive performance, it has been used in the face restoration methods [64, 175]. Li *et al.* [64] use the Swin Transformer blocks in the network to effectively extract latent facial features. Zhang *et al.* [175] integrate the Swin Transformer block into the UNet network to learn hierarchical facial features, achieving state-of-the-art performance in the face restoration task.

4.3 Loss Functions

To optimize face restoration networks, numerous loss functions have been proposed in the literature. In general, loss functions used in the existing methods can be approximately divided into pixel-wise loss, perceptual loss, adversarial loss, and face-specific loss. We review these representative loss functions in the following.

Pixel-wise Loss. The pixel-wise loss measures the pixel-wise difference between the recovered image and its corresponding clear image. It can quickly match the feature distribution of restored and clear images and speed up network

training. In existing methods, L1 and L2 losses are two widely-used pixel-wise losses in face restoration. They can be formulated as:

$$\mathcal{L}_1 = \frac{1}{CWH} \sum_{c=1}^C \sum_{x=1}^W \sum_{y=1}^H \|I_{hq}(x, y, c) - \hat{I}_{hq}(x, y, c)\|_1, \quad (11)$$

$$\mathcal{L}_2 = \frac{1}{CWH} \sum_{c=1}^C \sum_{x=1}^W \sum_{y=1}^H \|I_{hq}(x, y, c) - \hat{I}_{hq}(x, y, c)\|_2^2, \quad (12)$$

where I_{hq} and \hat{I}_{hq} represent the ground-truth and recovered face images respectively. W and H denote the size of the image. C refers to the channel of the image. It can be seen that L2 loss is only sensitive to large errors, while L1 loss treats larger and smaller errors equally. Early methods [6, 17, 55] usually use L2 loss in their models and recent works [141, 165, 182] mainly resort to L1 loss. While the pixel-wise loss can force the model to achieve high PSNR values, it often results in over-smooth and unrealistic images [6, 173].

Perceptual Loss. To generate more high-quality face images, methods [6, 55, 154, 181] adopt a perceptual loss to train the network. The perceptual loss [50] computes the difference between the recovered image and the ground-truth image in the feature space of a pre-trained deep network such as VGG16, VGG19 [113], and ResNet [34]. The perceptual loss over a deep pre-trained network features at a given layer i is shown as:

$$\mathcal{L}_{\text{per}} = \frac{1}{C_i W_i H_i} \sum_{c=1}^{C_i} \sum_{x=1}^{W_i} \sum_{y=1}^{H_i} \left(\phi_i(I_{hq}) - \phi_i(\hat{I}_{hq}) \right)^2, \quad (13)$$

where ϕ_i denotes the feature map obtained in the i -th layer of the pre-trained network, and W_i, H_i represent the shape of the feature map. C_i is the channel number. Benefiting from the perceptual loss, face restoration methods [6, 32, 165] generate visually-pleasing results.

Adversarial Loss. The objective of GAN-based face restoration methods [135, 150, 182] is based on the min-max game. The core idea is to learn a generator \mathcal{G} to generate a high-quality face image such that the discriminator \mathcal{D} cannot distinguish between the recovered image and the ground-truth image. This process can be expressed as solving the following min-max problem:

$$\begin{aligned} \min_{\mathcal{G}} \max_{\mathcal{D}} V(\mathcal{G}, \mathcal{D}) = & \mathbb{E}_{I_{hq} \sim p_{\text{train}}(I_{hq})} [\log(\mathcal{D}(I_{hq}))] + \\ & \mathbb{E}_{I_{lq} \sim p_{\mathcal{G}}(I_{lq})} [\log(1 - \mathcal{D}(\mathcal{G}(I_{lq})))], \end{aligned} \quad (14)$$

where I_{hq} and I_{lq} are the high-quality face image and low-quality input image. The adversarial loss from the discriminator to optimize the generator is formulated as:

$$\mathcal{L}_{\text{adv}} = \log(1 - \mathcal{D}(\mathcal{G}(I_{lq}))), \quad (15)$$

where $\mathcal{D}(\mathcal{G}(I_{lq}))$ is the probability that the restored image is close to the ground truth image. With the help of adversarial loss, existing face restoration methods [135, 149, 150, 182] can generate realistic textures in the recovered face image.

Face-specific Loss. As a highly structured object, the human face has its own special characteristics, thus some face-related losses are used in face restoration. This kind of loss aims at incorporating information related to the structure of the human face into the face restoration process. The widely-used one is heatmap loss [6, 55], which is

Table 1. Summary of benchmark datasets used in existing face restoration methods. – indicates that the resolution of the image is not fixed. HQ-LQ represents the pairs of low-quality and high-quality face images in the dataset.

Dataset	Size	Additional Label				Resolution	HQ-LQ
		Attributes	Landmarks	Parsing maps	Identity		
BioID [46]	1,521	✗	20	✗	✗	384 × 286	✗
LFW [45]	13,233	73	✗	✗	✓	250 × 250	✗
AFLW [57]	25,993	✗	21	✗	✗	–	✗
Helen [62]	2,330	✗	194	✓	✗	–	✗
300W [105]	3,837	✗	68	✗	✗	–	✗
300W-LP [185]	61,225	✗	✗	✗	✗	–	✗
LS3D-W [5]	230,000	✗	68	✗	✗	–	✗
LS3D-W balanced [5]	7,200	✗	68	✗	✗	–	✗
CASIA-WebFace [156]	494,414	✗	2	✗	✓	250 × 250	✗
CelebA [86]	202,599	40	5	✗	✓	–	✗
IMDB-WIKI [103]	524,230	✗	✗	✗	✗	–	✗
VGGFace [99]	2,600,000	✗	✗	✗	✓	–	✗
Menpo [168]	8,979	✗	68/39	✗	✗	–	✗
VGGFace2 [9]	3,310,000	✗	✗	✗	✓	–	✗
CelebA-HQ [52]	30,000	✗	5	✗	✗	1024 × 1024	✗
FFHQ [53]	70,000	✗	68	✗	✗	1024 × 1024	✗
EDFace-Celeb-1M [171]	1,700,000	✗	✗	✗	✗	–	✓
EDFace-Celeb-1M (BFR128) [175]	1,505,888	✗	✗	✗	✗	128 × 128	✓
EDFace-Celeb-150K (BFR512) [175]	148,962	✗	✗	✗	✗	512 × 512	✓

defined as:

$$\mathcal{L}_{\text{heatmap}} = \frac{1}{r^2 NWH} \sum_{n=1}^N \sum_{x=1}^{rW} \sum_{y=1}^{rH} \left(M_{x,y}^n - \tilde{M}_{x,y}^n \right)^2, \quad (16)$$

where N represents the number of landmarks, M and \tilde{M} are face heatmaps that are calculated from the ground-truths and restored images respectively. Some works introduce human identity loss in the model. The identity preserving loss [135] is shown as:

$$\mathcal{L}_{id} = \|\eta(\hat{I}_{hq}) - \eta(I_{hq})\|_1, \quad (17)$$

where η is a face feature extractor, e.g., ArcFace [21], which is used to capture features for identity discrimination. In addition, many other face-specific loss functions are proposed, including facial attention loss [55], face rendering loss [42], semantic-aware style loss [13], landmark loss [72], facial component loss [135], and parsing loss [110].

4.4 Datasets

To facilitate training and evaluation in face restoration, numerous benchmark datasets have been proposed. Table 1 summarizes the key datasets, which are detailed below. **BioID** [46] contains 1,521 grayscale images from 23 subjects. **LFW** [45] includes 13,233 images of 5,749 people and features more diverse content than BioID. **AFLW** [57] offers 25,993 images with up to 21 annotated landmarks per image, covering a wide range of poses and expressions. **Helen** [62] consists of 2,330 high-resolution images with 194 landmarks per face. **300W** [105] provides 3,837 images with 68-point annotations. Its extended version, **300W-LP** [185], contains 61,225 images rendered with varied poses. **LS3D-W** [5] offers about 230,000 face images with 3D landmarks; its balanced subset contains 7,200 images evenly distributed across pose ranges. **CASIA-WebFace** [156] comprises 494,414 face images of 10,575 subjects at 250 × 250 resolution. **CelebA** [86] contains 202,599 images from 10,177 identities, each annotated with 40 attributes and 5 key points. Based on it, **CelebA-Test** [70, 141] is synthesized with 3,000 CelebA-HQ images for model evaluation. **IMDB-WIKI** [103] provides 524,230 images sourced from IMDB (461,871) and Wikipedia (62,359). **VGGFace** [99] includes 2.6 million

images from 2,622 identities. **Menpo** [168] has 8,979 images with either 68-point or 39-point landmarks depending on visibility. **VGGFace2** [9] contains 3.31 million images of 9,131 subjects, with diverse variations and manually validated bounding boxes. **CelebA-HQ** [52] is a high-resolution (1024×1024) version of CelebA. **FFHQ** [53] consists of 70,000 high-quality images from Flickr, covering diverse demographics and accessories. **EDFace-Celeb-1M** [171] contains 1.7M images with racial diversity, offering 1.5M paired low-/high-resolution images and 140K real-world tiny faces for evaluation. **EDFace-Celeb-1M (BFR128)** [175] is designed for blind face restoration with synthetic degradations (blur, noise, low resolution, JPEG artifacts, and combinations), containing 1.5M images (128 × 128) across multiple tasks. **EDFace-Celeb-150K (BFR512)** [175] shares similar degradation settings with BFR128 but features 149K higher-resolution images (512 × 512), with 132K for training and 17K for testing.

5 PERFORMANCE EVALUATION

5.1 Representative Methods

To better understand the landscape of deep learning-based face restoration, we evaluate a diverse set of recent methods across both synthetic datasets (EDFace-Celeb-1M (BFR128) [175], EDFace-Celeb-150K (BFR512) [175], CelebA-Test [86], CelebA-HQ [52], FFHQ [53]) and real-world datasets (LFW-Test [45], CelebChild [135], WebPhoto [135]). The selected methods span various categories and have publicly available code.

GAN-based methods: TDTN [127] uses a triple domain translation network for old photo restoration. DFDNet [70] leverages facial dictionaries for reference-based restoration. mGANprior [32] applies GAN inversion via multi-latent code sampling. HiFaceGAN [149] employs hierarchical semantic guidance. PULSE [91] restores via latent space exploration. PSFR-GAN [13], GPEN [150], and GFP-GAN [135] are recent GAN-based state-of-the-art frameworks.

Transformer-based methods: STUNet [175] and RestoreFormer [141] introduce Transformer structures with spatial attention for blind face restoration. CodeFormer [181] predicts discrete latent codes for high-fidelity reconstruction.

Other learning paradigms: VQFR [33] incorporates vector quantization to guide detail recovery. DiffFace [166] introduces a diffusion-based framework for blind restoration.

5.2 Experimental Setting and Metric

Setting. To provide a clear view of existing face restoration methods, we use both synthetic datasets (EDFace-Celeb-1M (BFR128) [175], EDFace-Celeb-150K (BFR512) [175], FFHQ [53], CelebA-HQ [52], and CelebA-Test [86]) and real-world datasets (LFW-Test, CelebChild-Test, and WebPhoto-Test [135]) for training and evaluation. Specifically, we conduct three distinct experimental settings for the purpose of model training and testing. The details of these settings are outlined below.

Experimental Scheme One: EDFace-Celeb-1M (BFR128) and EDFace-Celeb-150K (BFR512) provide five degradation settings corresponding to face deblurring, face denoising, face artifact removal, face super-resolution, and blind face restoration tasks. We adopt the code and pre-trained models provided in [175]. For a fair comparison, these methods are first trained with the same configurations (e.g., same number of epochs) on the training sets of EDFace-Celeb-1M (BFR128) and EDFace-Celeb-150K (BFR512) respectively. Then, the trained models are evaluated on the testing sets of EDFace-Celeb-1M (BFR128) and EDFace-Celeb-150K (BFR512) respectively.

Experimental Scheme Two: In [70, 135, 141], they first synthesize degraded face images on the FFHQ [53] dataset via the degradation model. In the degradation model, the parameters σ , δ , r and q are randomly sampled from $\{0.2 : 10\}$, $\{1 : 8\}$, $\{0 : 20\}$, and $\{60 : 100\}$, respectively. Then, they use paired face images to train networks. In addition, one

Table 2. Performance comparison among representative BFR methods. The training sets are EDFace-Celeb-1M (BFR128) and EDFace-Celeb-150K (BFR512) respectively. The best and the second best performance values are highlighted and underlined respectively. Note that DFDN can only generate 512×512 face results for any input image, thus we do not report its results on the EDFace-Celeb-1M (BFR128) dataset.

Task	Methods	EDFace-Celeb-1M (BFR128)					EDFace-Celeb-150K (BFR512)				
		PSNR↑	SSIM↑	MS-SSIM↑	LPIPS↓	NIQE↓	PSNR↑	SSIM↑	MS-SSIM↑	LPIPS↓	NIQE↓
Face Deblurring	DFDNet [70]	—	—	—	—	—	25.4072	0.6512	0.8724	0.4008	7.8913
	HiFaceGAN [149]	22.4598	0.7974	0.9420	0.0739	8.7261	26.7421	0.8095	0.9382	0.2029	16.6642
	PSFR-GAN [13]	29.1411	0.8563	0.9818	0.0480	9.0008	27.4023	0.7604	0.9155	0.2292	17.4076
	GFP-GAN [135]	25.3822	0.7461	0.9534	0.0704	12.3608	28.8166	0.7709	0.9180	<u>0.1721</u>	15.5942
	GPEN [150]	24.9091	0.7307	0.9500	0.0887	<u>8.2288</u>	27.0658	0.7175	0.8928	0.2188	15.3187
	RestoreFormer [141]	27.2223	0.7560	0.9587	0.0692	9.0112	28.7231	0.7519	0.9121	0.1825	15.3217
	VQFR [33]	27.3524	0.7989	0.9618	<u>0.0632</u>	8.1284	28.4513	0.7218	0.9001	0.1698	15.3019
	STUNet [175]	27.3912	0.8080	<u>0.9669</u>	0.2019	12.2652	29.5572	0.8052	<u>0.9289</u>	0.3381	14.7874
Face Denoising	DFDNet [70]	—	—	—	—	—	24.3618	0.5738	0.8423	0.3238	7.7809
	HiFaceGAN [149]	26.2976	0.8801	0.9663	0.0306	7.2432	30.0409	<u>0.8731</u>	0.9563	0.1439	16.7363
	PSFR-GAN [13]	<u>33.1007</u>	0.8563	0.9818	0.0480	9.0008	28.5397	0.8232	0.9390	0.2208	19.4719
	GFP-GAN [135]	31.1053	0.8802	0.9849	0.0234	<u>7.9522</u>	33.2020	0.8711	0.9582	0.1259	15.8440
	GPEN [150]	33.0744	<u>0.9086</u>	<u>0.9871</u>	<u>0.0211</u>	8.0616	32.3736	0.8517	0.9506	0.1555	15.6820
	RestoreFormer [141]	32.9817	0.8810	0.9852	0.0312	8.0412	33.1848	0.8698	0.9517	<u>0.1369</u>	15.1598
	VQFR [33]	33.0114	0.9001	0.9861	0.0208	7.9812	33.1247	0.8685	0.9498	0.1401	16.0212
	STUNet [175]	34.8914	0.9302	0.9900	0.0331	8.5349	34.5500	0.8848	0.9587	0.1787	16.5480
Face Artifact Removal	DFDNet [70]	—	—	—	—	—	27.4781	0.7845	0.9409	0.2241	7.5553
	HiFaceGAN [149]	23.8228	0.8531	0.9567	0.0453	7.6479	27.1164	0.8897	0.9635	0.1241	18.7117
	PSFR-GAN [13]	<u>31.9455</u>	0.8899	<u>0.9887</u>	0.0190	8.3158	29.4285	0.9101	0.9719	0.1245	15.9760
	GFP-GAN [135]	31.0910	0.8804	0.9874	<u>0.0227</u>	<u>7.8027</u>	<u>35.7201</u>	<u>0.9144</u>	<u>0.9780</u>	0.0842	16.8320
	GPEN [150]	30.5753	0.8556	0.9837	0.0241	7.8074	33.8355	0.8701	0.9657	0.0986	16.9854
	RestoreFormer [141]	30.9811	0.8798	0.9851	0.0231	7.8036	35.3147	0.9098	0.9710	0.1023	16.9134
	VQFR [33]	30.9711	0.8791	0.9843	0.0238	7.8051	35.2956	0.9038	0.9701	0.1192	16.9321
	STUNet [175]	33.2082	0.9171	0.9912	0.0582	10.5596	36.5017	0.9246	0.9799	0.1411	16.0487
Face Super-Resolution	DFDNet [70]	—	—	—	—	—	26.8691	0.7405	0.9224	0.2620	7.4796
	HiFaceGAN [149]	24.2965	<u>0.7792</u>	0.9493	0.0911	8.4801	26.6103	0.8480	0.9476	0.1681	15.8911
	PSFR-GAN [13]	23.9671	0.6858	0.9381	0.1364	7.4807	33.1233	0.8588	0.9602	<u>0.1331</u>	16.7143
	GFP-GAN [135]	<u>25.7118</u>	0.7558	0.9492	0.0762	11.4428	<u>33.4217</u>	<u>0.8629</u>	<u>0.9610</u>	0.1127	16.8970
	GPEN [150]	25.0208	0.7306	0.9448	<u>0.0843</u>	<u>7.9052</u>	31.3507	0.8273	0.9501	0.1357	<u>15.7813</u>
	RestoreFormer [141]	25.0609	0.7398	<u>0.9497</u>	0.0878	7.9671	33.1213	0.8580	0.9596	0.1353	15.8012
	VQFR [33]	25.0456	0.7387	0.9490	0.0897	7.9682	33.1028	0.8573	0.9590	0.1371	15.8023
	STUNet [175]	27.1206	0.8037	0.9566	0.2018	12.7177	33.9060	0.8809	0.9636	0.2235	17.0899
Blind Face Restoration	DFDNet [70]	—	—	—	—	—	23.9349	0.5573	0.8053	0.4231	9.0084
	HiFaceGAN [149]	22.2179	0.7088	0.9128	0.1528	9.6864	25.3083	0.7260	<u>0.8701</u>	0.3012	14.7883
	PSFR-GAN [13]	22.2620	0.5199	0.8811	0.3558	<u>8.3706</u>	26.2998	0.6934	0.8581	0.3167	17.1906
	GFP-GAN [135]	<u>23.4159</u>	0.6707	<u>0.9185</u>	0.1354	12.6364	28.4809	0.7857	0.9255	0.2171	14.4933
	GPEN [150]	22.9731	0.6348	0.9119	<u>0.1387</u>	8.0709	25.5778	0.6721	0.8448	0.3113	15.8422
	RestoreFormer [141]	23.4017	0.6891	0.9169	0.1360	8.4213	27.0114	0.7332	0.8632	0.4187	14.9811
	VQFR [33]	23.4001	0.6884	0.9168	0.1365	8.4229	27.0107	0.7308	0.8629	0.4205	14.9895
	STUNet [175]	24.5500	0.6978	0.9225	0.3523	13.0601	<u>27.1833</u>	<u>0.7346</u>	0.8654	0.4457	17.0305

synthetic dataset (CelebA-Test [86]) and three real-world datasets (LFW-Test, CelebChild-Test, and WebPhoto-Test [135]) are used as testing datasets to measure the performance of models. Note that these testing sets have no overlap with the FFHQ dataset.

Metric. The full-reference and non-reference metrics are employed to benchmark these methods in the experiments. The full-reference metrics contain PSNR, SSIM, MS-SSIM, and LPIPS. These full-reference metrics measure the visual quality in different aspects, including pixels, structure, and human perception. The non-reference metrics consist of NIQE and FID, which can be used for real-world datasets without ground truth.

Table 3. Quantitative comparisons on synthetic (CelebA-Test) and real-world datasets (LFW-Test, CelebChild-Test, WebPhoto-Test). Metrics include FID, PSNR, SSIM, LPIPS, and NIQE. The red and blue colors indicate the best and second-best performance, respectively. All models are trained or finetuned on face images synthesized from FFHQ [53].

Methods	CelebA-Test (Synthetic)				LFW-Test		CelebChild-Test		WebPhoto-Test	
	FID↓	PSNR↑	SSIM↑	LPIPS↓	FID↓	NIQE↓	FID↓	NIQE↓	FID↓	NIQE↓
Input	132.69	24.96	0.6624	0.4989	137.56	11.214	144.42	9.170	170.11	12.755
TDTN [127]	70.21	23.00	0.6189	0.4778	73.19	5.034	115.70	4.849	100.40	5.705
PULSE [91]	67.75	21.61	0.6287	0.4657	64.86	5.097	102.74	5.225	86.45	5.146
mGANprior [32]	82.27	24.30	0.6758	0.4584	73.00	6.051	126.54	6.841	120.75	7.226
DFDNet [70]	52.92	24.10	0.6092	0.4478	62.57	4.026	111.55	4.414	100.68	5.293
HiFaceGAN [149]	66.09	24.92	0.6195	0.4770	64.50	4.510	113.00	4.855	116.12	4.885
PSFR-GAN [13]	43.88	24.45	0.6308	0.4186	51.89	5.096	107.40	4.804	88.45	5.582
GFP-GAN [135]	42.39	24.46	0.6684	0.3551	49.96	3.882	111.78	4.349	87.35	4.144
RestoreFormer [141]	41.45	24.42	0.6404	0.3650	47.75	4.168	101.22	4.582	77.33	4.459
CodeFormer [181]	60.62	22.18	0.6104	0.2993	53.83	4.473	119.13	4.905	86.10	4.628
VQFR [33]	41.28	24.14	0.6360	0.3515	50.64	3.589	105.18	3.936	75.38	3.607
DiffFace [166]	18.27	24.08	0.7036	0.4354	45.23	3.834	96.47	4.394	85.52	4.043

5.3 Quantitative Evaluation

We evaluate several state-of-the-art face restoration methods on both the synthetic and real-world datasets quantitatively regarding tasks including face deblurring, face denoising, face artifact removal, face super-resolution, and blind face restoration.

Table 2 reports the quantitative results of eight face restoration methods on the EDFace-Celeb-1M and EDFace-Celeb-150K datasets, where face deblurring, face denoising, face artifact removal, face super-resolution, and blind face restoration refer to five face restoration tasks related to the degradation from blur, noise, JPEG, low resolution, and a mix of them, respectively. For the comparison results in terms of PSNR, SSIM, MS-SSIM, LPIPS, and NIQE, we have the following findings. (i) In terms of PSNR, SSIM, and MS-SSIM, the Transformer-based method STUNet is very competitive and outperforms the best face prior based methods. Specifically, STUNet achieves the best performance on face denoising, face artifact removal, and face super-resolution tasks, and it also achieves the second best performance in face deblurring and blind face restoration tasks. Compared with other face restoration methods (DFDNet, HiFaceGAN, PSFR-GAN, GFP-GAN, GPEN, RestorFormer, and VQFR), though STUNet does not explicitly consider the face-related prior, it still achieves outstanding performance in many face restoration tasks. It demonstrates that it is very important to choose a reasonable network architecture, and a well-designed architecture will easily result in stronger performance. This observation will inspire us to design deep networks based on a strong backbone network. (ii) In terms of LPIPS and NIQE (non-reference quantitative metrics), GFP-GAN and GPEN achieve the best or second best performance for most face tasks, and HiFaceGAN, PSFR-GAN, RestorFormer, and VQFR place the best or second best on some face tasks. Compared with STUNet, GAN-based methods (HiFaceGAN, PSFR-GAN, GFP-GAN, and GPEN) obtain better performance. Because GAN based methods are good at generating content pleasing the human visual perception system, easily achieving better performance on non-reference quantitative metrics. This suggests that we should consider more different metrics when carrying out the performance evaluation.

The quantitative results of the CelebA-Test [86] dataset are shown in Table 3, which includes a comprehensive evaluation of various state-of-the-art methods for blind face restoration. The comparison methods are TDTN, PULSE, mGANprior, DFDNet, HiFaceGAN, PSFR-GAN, RestorFormer, CodeFormer, VQFR, and the recent diffusion-based

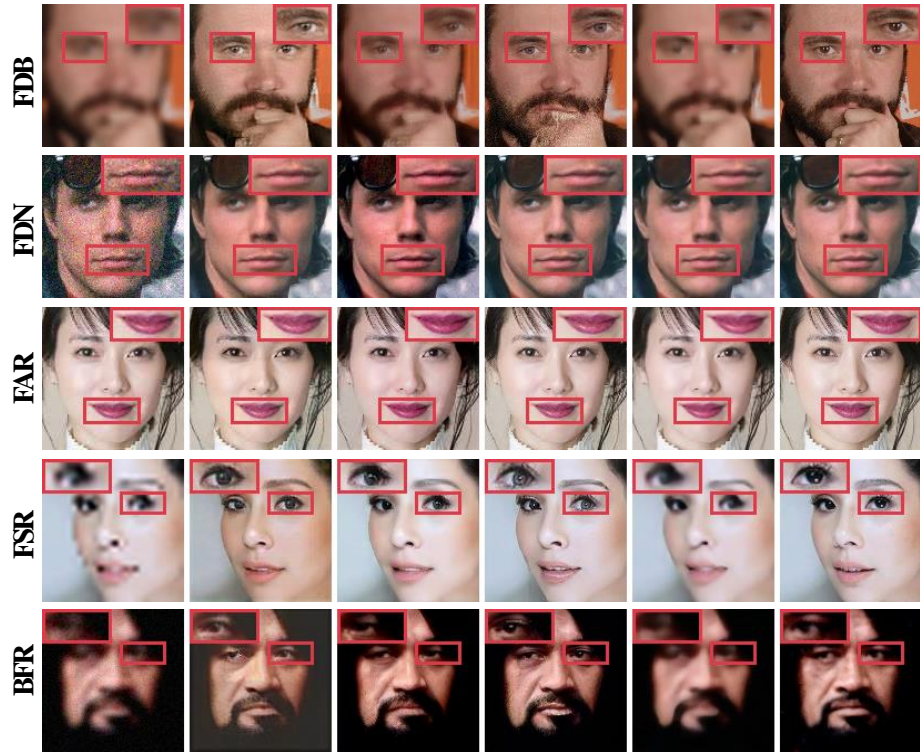


Fig. 11. Visual comparison on the **EDFace-Celeb-1M (BFR 128)** dataset. FDB, FDN, FAR, FSR, and BFR indicate face deblurring, face denoising, face artifact removal, face super-resolution, and face restoration, respectively. From left to right are the input, the results of HiFaceGAN, PSFR-GAN, GPEN, and STUNet, and HQ images.

method known as DiffFace. Among these methods, DiffFace and VQFR demonstrate competitive performance on the CelebA-Test dataset. Notably, DiffFace, as a diffusion-based method, achieves the highest performance in terms of FID and SSIM, signifying its superior ability in blind face restoration. VQFR, on the other hand, secures the second best performance in FID and LPIPS. Regarding PSNR, HiFaceGAN yields the highest performance, while GFP-GAN attains the second best performance. These results indicate that the reconstructed face images are more closely aligned with the ground-truth images in terms of pixel fidelity.

To evaluate the effectiveness of existing face restoration methods in real-world scenarios, we systematically assess their performance on three diverse real-world datasets: LFW-Test, CelebChild-Test, and WebPhoto-Test [135]. Table 3 reports the quantitative results in terms of FID and NIQE. VQFR, DiffFace, RestoreFormer, and GFP-GAN exhibit competitive performance in real-world face restoration. Specifically, VQFR achieves the highest performance on the WebPhoto-Test dataset and obtains the lowest NIQE scores across the LFW-Test and CelebChild-Test datasets. The superior performance of VQFR in real-world face image restoration can be attributed to its effective utilization of the vector quantization technique. Furthermore, the recent diffusion-based method, DiffFace, also demonstrates competitive performance in real-world scenes. DiffFace attains the best FID scores on both the LFW-Test and CelebChild-Test datasets while securing the second position in NIQE scores on the LFW-Test and WebPhoto-Test datasets. The evaluation

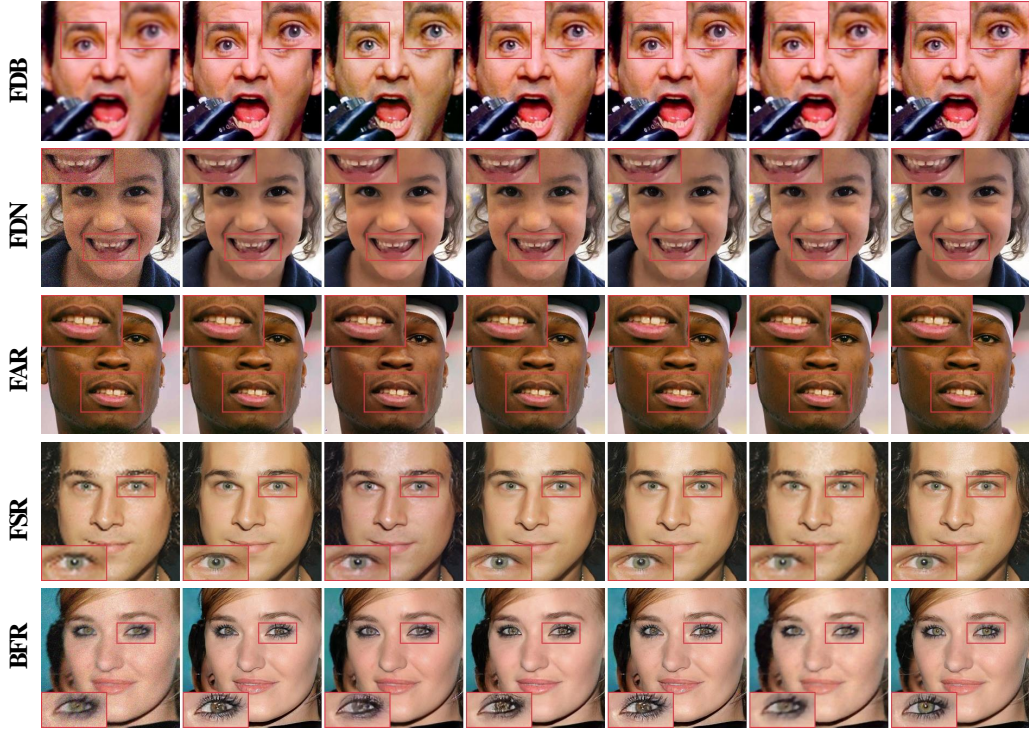


Fig. 12. Visual comparison on the **EDFace-Celeb-150K (BFR512)** dataset. FDB, FDN, FAR, FSR, and BFR indicate face deblurring, face denoising, face artifact removal, face super-resolution, and blind face restoration, respectively. From left to right are the input, the results of DDFDNet, HiFaceGAN, PSFR-GAN, GPEN, and STUNet, and HQ images.

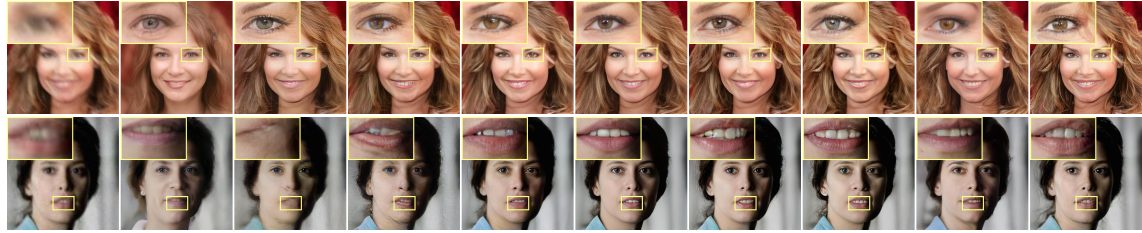


Fig. 13. Visual comparison on **CelebA-Test**. From left to right are the input, the results of PULSE, DFDNet, PSFR-GAN, GFP-GAN, CodeFormer, RestoreFormer, VQFR, DifFace, and HQ images.

of real-world datasets reveals that the vector quantization technique and recent diffusion model present promising directions for addressing real-world face restoration challenges. Additionally, the experiments demonstrate that FID and NIQE results do not always align. Hence, it is crucial to further explore face restoration performance evaluation metrics for future research.

Table 4. Running time and overhead comparison of typical face restoration methods. The number of parameters (Param) and multiply-accumulate operations (MACs) are used to compute the overhead. MACs are measured on 512×512 images. We test models with a PC using an NVIDIA GeForce 3090 GPU for fair comparisons.

Method	DFDNet [70]	HiFaceGAN [149]	PSFR-GAN [13]	VQFR [33]	TDTN [127]
Speed (sec.)	0.66	0.16	0.04	0.17	0.15
Params (M)	133.34	130.54	45.69	71.83	97.51
MACs (G)	608.74	697.70	102.80	1067.18	767.04
GFP-GAN [135]	GPEN [150]	STUNet [175]	RestoreFormer [141]	CodeFormer [181]	DifFace [166]
0.06	0.04	0.17	0.06	0.04	11.38
60.76	26.23	24.81	72.37	73.57	159.70
85.04	17.78	334.25	340.80	292.35	185.95

5.4 Qualitative Evaluation

Fig. 11 and Fig. 12 show some visual results of face deblurring, face denoising, face artifact removal, face super-resolution, and blind face restoration on EDFace-Celeb-1M and EDFace-Celeb-150K datasets, respectively. We can see that face images generated by the GAN-based methods (DFDNet, HiFaceGAN, PSFR-GAN, and GPEN) are more visually pleasing by human visual perception. For example, for face deblurring in the EDFace-Celeb-1M dataset, HiFaceGAN and GPEN can effectively remove the blur in face images, STUNet cannot deal with the blur well (see the eyes in the first row of Fig. 11). For the most challenging task of blind face restoration, we find that GPEN generates visually more pleasing face images (see the woman’s eyes in the last row of Fig. 12). The visual results are more consistent with the results of the non-reference metrics. Therefore, non-reference indicators (e.g., NIQE, FID) should be fully considered in the performance evaluation.

Fig. 13 presents the visual results on the set of CelebA-Test. In the figure, PULSE can recover face images well. However, it changes the human identity compared with GFP-GAN and RestoreFormer. DFDNet and PSFR-GAN cannot recover details of faces well (see the left eye in the first row and the mouth marked yellow box in the second row). The recent state-of-the-art methods RestoreFormer, VQFR, and DifFace can generate plausible face images.

We also evaluate the generalization ability of several representative face restoration methods on real-world datasets: LFW-Test, CelebChild-Test, and WebPhoto-Test. The qualitative comparisons are presented in Fig. 14. Among the evaluated methods, GFP-GAN, RestoreFormer, and DifFace demonstrate the capability to generate realistic faces in complex real-world scenes. For instance, GFP-GAN effectively enhances color and restores sharp details, such as the woman’s mouth in the fifth row and the child’s eye in the fourth row, in comparison to all other methods. While the recent diffusion-based method DifFace successfully recovers face images, it struggles to control the facial attributes in the resulting images, as evidenced by the issue with the girl’s eye in the last row of comparisons. Overall, GFP-GAN with generative face priors demonstrates superior generalization ability in real-world scenarios. Recent Transformer and diffusion models place a latent direction for real-world face restoration. On the other hand, there is still a need to develop new techniques and models to effectively address the challenges in real-world face restoration.

5.5 Computational Complexity

To provide a more comprehensive analysis of the time and complexity of existing face restoration methods, we choose seventeen representative face methods for comparison. These methods include DFDNet [70], HiFaceGAN [149], PSFR-GAN [13], VQFR [33], TDTN [127], GFP-GAN [135], GPEN [150], STUNet [175], RestoreFormer [141], CodeFormer [181], and DifFace [166]. Table 4 shows the running time and overhead of the existing state-of-the-art methods. All methods



Fig. 14. Visual comparison on **real-world LFW-Test**, **CelebChild-Test**, **WebPhoto-Test** datasets. From left to right are the input, the results of HiFaceGAN, DFDNet, PSFR-GAN, PULSE, GFP-GAN, RestoreFormer, CodeFormer, VQFR, and DiffFace.

are implemented in the same computer using one GPU. Our analysis of the results reveals that LaMa and GMCNN exhibit faster inference speeds compared to other methods, and CA employs the fewest parameters. However, the existing diffusion-based method DiffFace has a longer inference duration compared to the end-to-end face restoration network. In addition to GPEN, other methods have high computational complexity (see MACs). Some Transformer-based methods, such as STUNet, RestoreFormer, and CodeFormer have higher computational complexity than CNN-based methods. In general, the majority of the existing state-of-the-art face restoration methods are complex. In the future, we expect more work on developing lightweight face restoration models for edge devices.

6 FUTURE DIRECTIONS

Despite great breakthroughs in face restoration technology, there still exist many challenges and unsolved problems. In this section, we discuss the limitations of existing methods and introduce new trends for future work.

Network Design. As discussed in the performance evaluation, the network structure can significantly influence the restoration performance. For example, recent Transformer-based methods usually have better performance due to the strong ability of Transformer architecture. GAN-based methods can generate visually pleasing face images with better non-reference metric values. Thus, when designing the network, it is worthwhile to learn from different structures, including CNN, GAN, ViT, and diffusion models. On the other hand, recent Transformer-based models typically necessitate high computational costs and larger parameter sizes, while diffusion-based models suffer from slow

inference speeds, rendering them less conducive for deployment on edge devices. Thus, how to design a lightweight network with strong performance is another potential research direction for future work.

Integration of Facial Priors and Networks. As a domain-specific image restoration task, the facial features can be used in the face restoration task. When designing models, many methods aim at exploiting facial priors to recover realistic face details. Although some methods attempt to introduce geometry prior, facial component, generative prior, or 3D prior into face restoration, how to integrate the prior information into networks is still a promising direction for this task. In addition, exploiting new face-related priors such as priors from pre-trained GAN/diffusion-based models or data statistics in networks, is another direction for this task.

Loss Function and Evaluation Metrics. For the face restoration task, different loss functions have been adopted in the literature. The widely-used loss functions are L1 loss, L2 loss, perceptual loss, adversarial loss, and face-specific loss. Instead of using a single loss function, existing methods usually combine multiple loss functions with corresponding weights to train models. However, it is still not clear how to develop the right loss function for guiding the model training. Thus, in the future, more works are expected to seek more accurate loss functions (e.g., general or task-driven loss functions) to promote the development of face restoration. In addition, loss functions can directly influence the evaluation results of models. As shown in Table 2 and 3, the pixel-wise L1 loss and L2 Loss tend to obtain better results in terms of PSNR, SSIM, and MS-SSIM. The perceptual loss and adversarial loss tend to generate more visual-pleasing results (*i.e.*, producing high LPIPS, FID, and NIQE values). Thus, how to develop metrics that can consider both human and machine aspects for model evaluation is also an important direction in the future.

Computational Cost. Existing face restoration methods aim at improving the restoration performance by significantly increasing the depth or width of the network, ignoring the computational cost of models. The heavy computational cost prevents these methods from being used in resource-limited environments, such as mobile or embedded devices. For example, as shown in Table 4, the state-of-the-art method RestoreFormer [141] has 72.37M parameters and 340.80G MACs. The diffusion-based method DiffFace suffers from a longer inference speed. It is very difficult to deploy them in real-world applications. Therefore, developing models with a lighter computational cost is an important future direction.

Standard Benchmark Datasets. Unlike other low-level visual tasks such as image deblurring, image denoising, and image dehazing, there are few standard evaluation benchmarks for face restoration [175]. For example, most face restoration methods [70, 135, 141] conduct experiments on private datasets (synthesizing the training set from FFHQ). Researchers may tend to use data that is biased to their proposed methods. On the other hand, to make a fair comparison, subsequent works need to take a lot of time to synthesize private data sets and retrain other comparison methods. In addition, the scale of the recent widely-used dataset is usually small, which is not suitable for deep learning methods. Thus, developing standard benchmark datasets is a direction for the face restoration task. In the future, we expect more standard and high-quality benchmark datasets to be built by researchers in the community.

Video Face Restoration. With the popularization of mobile phones and cameras, the video face restoration task has become more and more important. However, existing works mainly focus on image-level face restoration, and there are few video-related works for face restoration. On the other hand, other low-level visual tasks such as video deblurring, video super-resolution, and video denoising have developed rapidly in recent years. Therefore, video face restoration is a potential direction for the community. The task of video face restoration can be considered from the following two aspects. First, for the benchmark dataset, we could consider building high-quality video datasets for this task, which can quickly facilitate algorithm design and evaluation and benefit the community of face restoration. Second, for video restoration methods, we should develop video-based face restoration by fully considering the spatial and temporal information among successive frames.

Real-world Face Restoration and Application. Existing methods rely on synthetic data to train networks. However, the trained networks cannot necessarily perform well in real-world scenarios. As shown in Table 3 and Fig. 14, most face restoration methods produce poor results when dealing with real-world face images. Because there is a natural domain gap between synthetic data and real-world data. Some solutions are introduced to solve this problem, such as unsupervised techniques or learning real image degradation techniques. However, they still rely on some specific assumptions that all images have similar degradation. Thus, the real-world application is still a challenging direction for the task of face restoration. In addition, some methods [49, 110] have shown that face restoration can improve the performance of subsequent tasks such as face verification and face recognition. However, how to couple face restoration with these tasks in a framework is a future research direction.

Other Related Tasks. In addition to the above-discussed face restoration tasks, there are many tasks related to face restoration, including face retouching [63, 107], photo-sketch synthesis [160, 183], face-to-face translation [58, 153], color enhancement [47, 181], and old photo restoration [127, 128]. For example, face retouching entails digitally enhancing facial features and appearance in photographs to create a more attractive and polished look. The goal of face retouching is to attain smoother skin, enhance complexion, improve the appearance of the eyes and teeth, and make adjustments to hair, makeup, and facial proportions. Old photo restoration is the task of repairing old photos, where the degradation of old photos is rather diverse and complex (e.g., noise, blur, and color fading). In addition, some tasks focus on facial style transfer, such as face-to-face translation and facial expression analysis, which are different from face restoration. Thus, applying the existing face restoration methods to these related tasks is also a promising direction, which can trigger more applications to land.

7 CONCLUSION

In this work, we have systematically surveyed face restoration methods using deep learning. We discuss different degradation models, the characteristics of face images, the challenges of face restoration, and the core ideas in existing state-of-the-art methods, including geometric prior based methods, reference prior based methods, generative prior based methods, and non-prior based methods. After comprehensively reviewing face restoration methods, we discuss advanced techniques in face recovery methods from aspects of network architecture, basic block, loss function, and benchmark dataset. We also evaluate the representative methods on synthetic and real-world datasets. Finally, we discuss the future directions, including network design, metrics, benchmark datasets, applications, *etc.*

REFERENCES

- [1] Saeed Anwar and Nick Barnes. 2019. Real image denoising with feature attention. In *ICCV*.
- [2] Saeed Anwar, Fatih Porikli, and Cong Phuoc Huynh. 2017. Category-specific object image denoising. *TIP* (2017).
- [3] Simon Baker and Takeo Kanade. 2000. Hallucinating faces. In *FG*.
- [4] Qiqi Bao, Yunmeng Liu, Bowen Gang, Wenming Yang, and Qingmin Liao. 2023. SCTANet: A Spatial Attention-Guided CNN-Transformer Aggregation Network for Deep Face Image Super-Resolution. *TMM* (2023).
- [5] Adrian Bulat and Georgios Tzimiropoulos. 2017. How far are we from solving the 2d & 3d face alignment problem?(and a dataset of 230,000 3d facial landmarks). In *ICCV*.
- [6] Adrian Bulat and Georgios Tzimiropoulos. 2018. Super-fan: Integrated facial landmark localization and super-resolution of real-world low resolution faces in arbitrary poses with gans. In *CVPR*.
- [7] Adrian Bulat, Jing Yang, and Georgios Tzimiropoulos. 2018. To learn image super-resolution, use a gan to learn how to do image degradation first. In *ECCV*.
- [8] Qingxing Cao, Liang Lin, Yukai Shi, Xiaodan Liang, and Guanbin Li. 2017. Attention-aware face hallucination via deep reinforcement learning. In *CVPR*.
- [9] Qiong Cao, Li Shen, Weidi Xie, Omkar M Parkhi, and Andrew Zisserman. 2018. Vggface2: A dataset for recognising faces across pose and age. In *FG*.

- [10] Nicolas Carion, Francisco Massa, Gabriel Synnaeve, Nicolas Usunier, Alexander Kirillov, and Sergey Zagoruyko. 2020. End-to-end object detection with transformers. In *ECCV*.
- [11] Ahmed Cheikh Sidiya, Xuan Xu, Ning Xu, and Xin Li. 2023. Degradation learning and Skip-Transformer for blind face restoration. *Frontiers in Signal Processing* 3 (2023), 1106465.
- [12] Chaofeng Chen, Dihong Gong, Hao Wang, Zhifeng Li, and Kwan-Yee K Wong. 2020. Learning spatial attention for face super-resolution. *TIP* (2020).
- [13] Chaofeng Chen, Xiaoming Li, Lingbo Yang, Xianhui Lin, Lei Zhang, and Kwan-Yee K Wong. 2021. Progressive semantic-aware style transformation for blind face restoration. In *CVPR*.
- [14] Chenyi Chen, Ari Seff, Alain Kornhauser, and Jianxiong Xiao. 2015. Deepdriving: Learning affordance for direct perception in autonomous driving. In *ICCV*.
- [15] Jin Chen, Jun Chen, Zheng Wang, Chao Liang, and Chia-Wen Lin. 2020. Identity-aware face super-resolution for low-resolution face recognition. *IEEE Signal Processing Letters* (2020).
- [16] Shu-Jie Chen and Hui-Liang Shen. 2015. Multispectral image out-of-focus deblurring using interchannel correlation. *TIP* (2015).
- [17] Yu Chen, Ying Tai, Xiaoming Liu, Chunhua Shen, and Jian Yang. 2018. Fsrnet: End-to-end learning face super-resolution with facial priors. In *CVPR*.
- [18] Vishal Chudasama, Kartik Nighania, Kishor Upala, Kiran Raja, Raghavendra Ramachandra, and Christoph Busch. 2021. E-comsupresnet: Enhanced face super-resolution through compact network. *T-BIOM* (2021).
- [19] Antonia Creswell, Tom White, Vincent Dumoulin, Kai Arulkumaran, Biswa Sengupta, and Anil A Bharath. 2018. Generative adversarial networks: An overview. *IEEE Signal Processing Magazine* (2018).
- [20] Jiankang Deng, Jia Guo, Evangelos Ververas, Irene Kotsia, and Stefanos Zafeiriou. 2020. Retinaface: Single-shot multi-level face localisation in the wild. In *CVPR*.
- [21] Jiankang Deng, Jia Guo, Niannan Xue, and Stefanos Zafeiriou. 2019. Arcface: Additive angular margin loss for deep face recognition. In *CVPR*.
- [22] Berk Dogan, Shuhang Gu, and Radu Timofte. 2019. Exemplar guided face image super-resolution without facial landmarks. In *CVPRW*.
- [23] Chao Dong, Yubin Deng, Chen Change Loy, and Xiaoou Tang. 2015. Compression artifacts reduction by a deep convolutional network. In *ICCV*.
- [24] Chao Dong, Chen Change Loy, Kaiming He, and Xiaoou Tang. 2015. Image super-resolution using deep convolutional networks. *TPAMI* (2015).
- [25] Xuanyi Dong, Yan Yan, Wanli Ouyang, and Yi Yang. 2018. Style aggregated network for facial landmark detection. In *CVPR*.
- [26] Marcelo Dos Santos, Rayson Laroca, Rafael O Ribeiro, João Neves, Hugo Proen  a, and David Menotti. 2022. Face super-resolution using stochastic differential equations. In *SIBGRAPI*. 216–221.
- [27] Alexey Dosovitskiy, Lucas Beyer, Alexander Kolesnikov, Dirk Weissenborn, Xiaohua Zhai, Thomas Unterthiner, Mostafa Dehghani, Matthias Minderer, Georg Heigold, Sylvain Gelly, et al. 2021. An image is worth 16x16 words: Transformers for image recognition at scale. In *ICLR*.
- [28] Guangwei Gao, Zixiang Xu, Juncheng Li, Jian Yang, Tieyong Zeng, and Guo-Jun Qi. 2023. Ctcnet: A cnn-transformer cooperation network for face image super-resolution. *TIP* 32 (2023), 1978–1991.
- [29] Juhao Gao, Ni Tang, and Dongxiao Zhang. 2023. A Multi-Scale Deep Back-Projection Backbone for Face Super-Resolution with Diffusion Models. *Applied Sciences* 13, 14 (2023), 8110.
- [30] Ian Goodfellow, Jean Pouget-Abadie, Mehdi Mirza, Bing Xu, David Warde-Farley, Sherjil Ozair, Aaron Courville, and Yoshua Bengio. 2014. Generative adversarial nets. In *NeurIPS*.
- [31] Klemen Grm, Walter J Scheirer, and Vitomir   truc. 2019. Face hallucination using cascaded super-resolution and identity priors. *TIP* (2019).
- [32] Jinjin Gu, Yujun Shen, and Bolei Zhou. 2020. Image processing using multi-code gan prior. In *CVPR*.
- [33] Yuchao Gu, Xintao Wang, Liangbin Xie, Chao Dong, Gen Li, Ying Shan, and Ming-Ming Cheng. 2022. VQFR: Blind face restoration with vector-quantized dictionary and parallel decoder. In *ECCV*. 126–143.
- [34] Kaiming He, Xiangyu Zhang, Shaoqing Ren, and Jian Sun. 2016. Deep residual learning for image recognition. In *CVPR*.
- [35] Xiaofei He and Partha Niyogi. 2003. Locality preserving projections. In *NeurIPS*.
- [36] Martin Heusel, Hubert Ramsauer, Thomas Unterthiner, Bernhard Nessler, and Sepp Hochreiter. 2017. Gans trained by a two time-scale update rule converge to a local nash equilibrium. In *NeurIPS*.
- [37] Jonathan Ho, Ajay Jain, and Pieter Abbeel. 2020. Denoising diffusion probabilistic models. In *NIPS*. 6840–6851.
- [38] Alain Hore and Djemel Ziou. 2010. Image quality metrics: PSNR vs. SSIM. In *ICCV*.
- [39] Tobias Ho  feld, Poul E Heegaard, Mart  n Varela, and Sebastian M  ller. 2016. QoE beyond the MOS: an in-depth look at QoE via better metrics and their relation to MOS. *Quality and User Experience* (2016).
- [40] Hao Hou, Jun Xu, Yingkun Hou, Xiaotao Hu, Benzheng Wei, and Dinggang Shen. 2023. Semi-cycled generative adversarial networks for real-world face super-resolution. *TIP* 32 (2023), 1184–1199.
- [41] Jie Hu, Li Shen, and Gang Sun. 2018. Squeeze-and-excitation networks. In *CVPR*.
- [42] Xiaobin Hu, Wenqi Ren, Jiaolong Yang, Xiaochun Cao, David P Wipf, Bjoern Menze, Xin Tong, and Hongbin Zha. 2021. Face Restoration via Plug-and-Play 3D Facial Priors. *TPAMI* (2021).
- [43] Yujie Hu, Yinhua Wang, and Jian Zhang. 2023. Dear-gan: Degradation-aware face restoration with gan prior. *TCSVT* (2023).
- [44] Gao Huang, Zhuang Liu, Laurens Van Der Maaten, and Kilian Q Weinberger. 2017. Densely connected convolutional networks. In *CVPR*.

[45] Gary B Huang, Marwan Mattar, Tamara Berg, and Eric Learned-Miller. 2008. Labeled faces in the wild: A database for studying face recognition in unconstrained environments. In *Proceedings of Workshop on Faces in 'Real-Life' Images: Detection, Alignment, and Recognition*.

[46] Oliver Jesorsky, Klaus J Kirchberg, and Robert W Frischholz. 2001. Robust face detection using the hausdorff distance. In *AVBPA*.

[47] Xiaozhong Ji, Boyuan Jiang, Donghao Luo, Guangpin Tao, Wenqing Chu, Zhifeng Xie, Chengjie Wang, and Ying Tai. 2022. ColorFormer: Image Colorization via Color Memory Assisted Hybrid-Attention Transformer. In *ECCV*. 20–36.

[48] Junjun Jiang, Chenyang Wang, Xianming Liu, and Jiayi Ma. 2021. Deep learning-based face super-resolution: A survey. *Comput. Surveys* (2021).

[49] Kui Jiang, Zhongyuan Wang, Peng Yi, Tao Lu, Junjun Jiang, and Zixiang Xiong. 2020. Dual-path deep fusion network for face image hallucination. *TNNLS* (2020).

[50] Justin Johnson, Alexandre Alahi, and Li Fei-Fei. 2016. Perceptual losses for real-time style transfer and super-resolution. In *ECCV*.

[51] Ratheesh Kalarot, Tao Li, and Fatih Porikli. 2020. Component attention guided face super-resolution network: Cagface. In *WACV*.

[52] Tero Karras, Timo Aila, Samuli Laine, and Jaakko Lehtinen. 2018. Progressive Growing of GANs for Improved Quality, Stability, and Variation. In *ICLR*.

[53] Tero Karras, Samuli Laine, and Timo Aila. 2019. A style-based generator architecture for generative adversarial networks. In *CVPR*.

[54] Tero Karras, Samuli Laine, Miika Aittala, Janne Hellsten, Jaakko Lehtinen, and Timo Aila. 2020. Analyzing and improving the image quality of stylegan. In *CVPR*.

[55] Deokyun Kim, Minseon Kim, Gihyun Kwon, and Dae-Shik Kim. 2019. Progressive face super-resolution via attention to facial landmark. In *BMVC*.

[56] Jonghyun Kim, Gen Li, Cheolkon Jung, and Joongkyu Kim. 2021. Progressive Face Super-Resolution with Non-Parametric Facial Prior Enhancement. In *ICIP*.

[57] Martin Koestinger, Paul Wohlhart, Peter M Roth, and Horst Bischof. 2011. Annotated facial landmarks in the wild: A large-scale, real-world database for facial landmark localization. In *ICCVW*.

[58] Prajwal KR, Rudrabha Mukhopadhyay, Jerin Philip, Abhishek Jha, Vinay Namboodiri, and CV Jawahar. 2019. Towards automatic face-to-face translation. In *ACMMM*.

[59] Neeraj Kumar, Alexander C Berg, Peter N Belhumeur, and Shree K Nayar. 2009. Attribute and simile classifiers for face verification. In *ICCV*.

[60] Orest Kupyn, Volodymyr Budzan, Mykola Mykhailych, Dmytro Mishkin, and Jiří Matas. 2018. Deblurgan: Blind motion deblurring using conditional adversarial networks. In *CVPR*.

[61] Wei-Sheng Lai, Yichang Shih, Lun-Cheng Chu, Xiaotong Wu, Sung-Fang Tsai, Michael Krainin, Deqing Sun, and Chia-Kai Liang. 2022. Face deblurring using dual camera fusion on mobile phones. *ACM TOG* 41, 4 (2022), 1–16.

[62] Vuong Le, Jonathan Brandt, Zhe Lin, Lubomir Bourdev, and Thomas S Huang. 2012. Interactive facial feature localization. In *ECCV*.

[63] Biwen Lei, Xiefan Guo, Hongyu Yang, Miaoqiao Cui, Xuansong Xie, and Di Huang. 2022. ABPN: Adaptive Blend Pyramid Network for Real-Time Local Retouching of Ultra High-Resolution Photo. In *CVPR*. 2108–2117.

[64] Ajin Li, Gen Li, Lei Sun, and Xintao Wang. 2022. FaceFormer: Scale-aware Blind Face Restoration with Transformers. *arXiv preprint arXiv:2207.09790* (2022).

[65] Jingyuan Li, Ning Wang, Lefei Zhang, Bo Du, and Dacheng Tao. 2020. Recurrent feature reasoning for image inpainting. In *CVPR*. 7760–7768.

[66] Ke Li, Bahetiyaer Bare, Bo Yan, Bailan Feng, and Chunfeng Yao. 2018. Face hallucination based on key parts enhancement. In *ICASSP*.

[67] Mengyan Li, Zhaoyu Zhang, Jun Yu, and Chang Wen Chen. 2020. Learning face image super-resolution through facial semantic attribute transformation and self-attentive structure enhancement. *TIP* (2020).

[68] Stan Z Li and ZhenQiu Zhang. 2004. Floatboost learning and statistical face detection. *TPAMI* (2004).

[69] Wenbo Li, Zhe Lin, Kun Zhou, Lu Qi, Yi Wang, and Jiaya Jia. 2022. Mat: Mask-aware transformer for large hole image inpainting. In *CVPR*. 10758–10768.

[70] Xiaoming Li, Chaofeng Chen, Shangchen Zhou, Xianhui Lin, Wangmeng Zuo, and Lei Zhang. 2020. Blind face restoration via deep multi-scale component dictionaries. In *ECCV*.

[71] Xiaoming Li, Wenyu Li, Dongwei Ren, Hongzhi Zhang, Meng Wang, and Wangmeng Zuo. 2020. Enhanced blind face restoration with multi-exemplar images and adaptive spatial feature fusion. In *CVPR*.

[72] Xiaoming Li, Ming Liu, Yuting Ye, Wangmeng Zuo, Liang Lin, and Ruigang Yang. 2018. Learning warped guidance for blind face restoration. In *ECCV*.

[73] Xiaoming Li, Shiguang Zhang, Shangchen Zhou, Lei Zhang, and Wangmeng Zuo. 2022. Learning Dual Memory Dictionaries for Blind Face Restoration. *TPAMI* (2022).

[74] Yung-hui Li, Marios Savvides, and Vijayakumar Bhagavatula. 2006. Illumination tolerant face recognition using a novel face from sketch synthesis approach and advanced correlation filters. In *ICASSP*.

[75] Jingyun Liang, Jiezheng Cao, Guolei Sun, Kai Zhang, Luc Van Gool, and Radu Timofte. 2021. Swinir: Image restoration using swin transformer. In *ICCVW*. 1833–1844.

[76] Yan Liang, Jian-Huang Lai, Wei-Shi Zheng, and Zemin Cai. 2012. A survey of face hallucination. In *CCBR*.

[77] Bee Lim, Sanghyun Son, Heewon Kim, Seungjun Nah, and Kyoung Mu Lee. 2017. Enhanced deep residual networks for single image super-resolution. In *CVPRW*.

[78] Guilin Liu, Fitsum A Reda, Kevin J Shih, Ting-Chun Wang, Andrew Tao, and Bryan Catanzaro. 2018. Image inpainting for irregular holes using partial convolutions. In *ECCV*. 85–100.

[79] Heng Liu, Xiaoyu Zheng, Jungong Han, Yuezhong Chu, and Tao Tao. 2019. Survey on GAN-based face hallucination with its model development. *IET Image Processing* (2019).

[80] Jixin Liu, Rui Chen, Shipeng An, and Heng Zhang. 2021. CG-GAN: Class-Attribute Guided Generative Adversarial Network for Old Photo Restoration. In *ACMMM*.

[81] Jiaying Liu, Dong Liu, Wenhan Yang, Sifeng Xia, Xiaoshuai Zhang, and Yuanying Dai. 2020. A comprehensive benchmark for single image compression artifact reduction. *TIP* (2020).

[82] Lixiong Liu, Bao Liu, Hua Huang, and Alan Conrad Bovik. 2014. No-reference image quality assessment based on spatial and spectral entropies. *Signal Processing: Image Communication* (2014).

[83] Siyu Liu, Zheng-Peng Duan, Jia OuYang, Jiayi Fu, Hyunhee Park, Zikun Liu, Chun-Le Guo, and Chongyi Li. 2025. FaceMe: Robust blind face restoration with personal identification. In *AAAI*. 5567–5575.

[84] Ying Liu, Zhanlong Dong, Keng Pang Lim, and Nam Ling. 2020. A densely connected face super-resolution network based on attention mechanism. In *ISIEA*.

[85] Ze Liu, Yutong Lin, Yue Cao, Han Hu, Yixuan Wei, Zheng Zhang, Stephen Lin, and Baining Guo. 2021. Swin transformer: Hierarchical vision transformer using shifted windows. In *ICCV*.

[86] Ziwei Liu, Ping Luo, Xiaogang Wang, and Xiaou Tang. 2015. Deep learning face attributes in the wild. In *ICCV*.

[87] Tao Lu, Yuanzhi Wang, Yanduo Zhang, Yu Wang, Liu Wei, Zhongyuan Wang, and Junjun Jiang. 2021. Face hallucination via split-attention in split-attention network. In *ACMMM*.

[88] Wanglong Lu, Jikai Wang, Tao Wang, Kaihao Zhang, Xianta Jiang, and Hanli Zhao. 2025. Visual style prompt learning using diffusion models for blind face restoration. *PR* 161 (2025), 111312.

[89] Enming Luo, Stanley H Chan, and Truong Q Nguyen. 2015. Adaptive image denoising by targeted databases. *TIP* (2015).

[90] Cheng Ma, Zhenyu Jiang, Yongming Rao, Jiwen Lu, and Jie Zhou. 2020. Deep face super-resolution with iterative collaboration between attentive recovery and landmark estimation. In *CVPR*.

[91] Sachit Menon, Alexandru Damian, Shijia Hu, Nikhil Ravi, and Cynthia Rudin. 2020. Pulse: Self-supervised photo upsampling via latent space exploration of generative models. In *CVPR*.

[92] Anish Mittal, Anush Krishna Moorthy, and Alan Conrad Bovik. 2012. No-reference image quality assessment in the spatial domain. *TIP* (2012).

[93] Anish Mittal, Rajiv Soundararajan, and Alan C Bovik. 2012. Making a “completely blind” image quality analyzer. *IEEE Signal Processing Letters* (2012).

[94] Volodymyr Mnih, Nicolas Heess, Alex Graves, et al. 2014. Recurrent models of visual attention. In *NeurIPS*.

[95] Anush Krishna Moorthy and Alan Conrad Bovik. 2010. A two-step framework for constructing blind image quality indices. *IEEE Signal Processing Letters* (2010).

[96] Anush Krishna Moorthy and Alan Conrad Bovik. 2011. Blind image quality assessment: From natural scene statistics to perceptual quality. *TIP* (2011).

[97] Nithin Gopalakrishnan Nair, Kangfu Mei, and Vishal M Patel. 2023. At-ddpm: Restoring faces degraded by atmospheric turbulence using denoising diffusion probabilistic models. In *WACV*. 3434–3443.

[98] Kien Nguyen, Clinton Fookes, Sridha Sridharan, Massimo Tistarelli, and Mark Nixon. 2018. Super-resolution for biometrics: A comprehensive survey. *PR* (2018).

[99] Omkar M Parkhi, Andrea Vedaldi, and Andrew Zisserman. 2015. Deep face recognition. In *BMVC*.

[100] Haoran Qi, Yuwei Qiu, Xing Luo, and Zhi Jin. 2023. An Efficient Latent Style Guided Transformer-CNN Framework for Face Super-Resolution. *TMM* (2023).

[101] Xinmin Qiu, Congying Han, ZiCheng Zhang, Bonan Li, Tiande Guo, and Xuecheng Nie. 2023. DiffBFR: Bootstrapping Diffusion Model Towards Blind Face Restoration. *arXiv preprint arXiv:2305.04517* (2023).

[102] Shyam Singh Rajput, KV Arya, Vinay Singh, and Vijay Kumar Bohat. 2018. Face hallucination techniques: A survey. In *PICT*. 1–6.

[103] Rasmus Rothe, Radu Timofte, and Luc Van Gool. 2015. Dex: Deep expectation of apparent age from a single image. In *ICCW*.

[104] Michele A Saad, Alan C Bovik, and Christophe Charrier. 2012. Blind image quality assessment: A natural scene statistics approach in the DCT domain. *TIP* (2012).

[105] Christos Sagonas, Georgios Tzimiropoulos, Stefanos Zafeiriou, and Maja Pantic. 2013. 300 faces in-the-wild challenge: The first facial landmark localization challenge. In *ICCVW*.

[106] Chitwan Saharia, Jonathan Ho, William Chan, Tim Salimans, David J Fleet, and Mohammad Norouzi. 2022. Image super-resolution via iterative refinement. *TPAMI* 45, 4 (2022), 4713–4726.

[107] Alireza Shafaei, James J Little, and Mark Schmidt. 2021. Autoretouch: Automatic professional face retouching. In *WACV*.

[108] Wen-Ze Shao, Jing-Jing Xu, Long Chen, Qi Ge, Li-Qian Wang, Bing-Kun Bao, and Hai-Bo Li. 2019. On potentials of regularized Wasserstein generative adversarial networks for realistic hallucination of tiny faces. *Neurocomputing* (2019).

[109] Ziyi Shen, Wei-Sheng Lai, Tingfa Xu, Jan Kautz, and Ming-Hsuan Yang. 2018. Deep semantic face deblurring. In *CVPR*.

[110] Ziyi Shen, Wei-Sheng Lai, Tingfa Xu, Jan Kautz, and Ming-Hsuan Yang. 2020. Exploiting semantics for face image deblurring. *IJCV* (2020).

[111] Jingang Shi, Yusi Wang, Zitong Yu, Guanxin Li, Xiaopeng Hong, Fei Wang, and Yihong Gong. 2023. Exploiting Multi-scale Parallel Self-attention and Local Variation via Dual-branch transformer-CNN Structure for Face Super-resolution. *TMM* (2023).

- [112] Fatemeh Shiri, Xin Yu, Fatih Porikli, Richard Hartley, and Piotr Koniusz. 2019. Identity-preserving face recovery from stylized portraits. *IJCV* (2019).
- [113] Karen Simonyan and Andrew Zisserman. 2014. Very deep convolutional networks for large-scale image recognition. In *ICLR*.
- [114] Jascha Sohl-Dickstein, Eric Weiss, Niru Maheswaranathan, and Surya Ganguli. 2015. Deep unsupervised learning using nonequilibrium thermodynamics. In *ICML*. 2256–2265.
- [115] Jiaming Song, Chenlin Meng, and Stefano Ermon. 2020. Denoising Diffusion Implicit Models. In *ICLR*.
- [116] Jingwen Su, Boyan Xu, and Hujun Yin. 2022. A survey of deep learning approaches to image restoration. *Neurocomputing* (2022).
- [117] Roman Suvorov, Elizaveta Logacheva, Anton Mashikhin, Anastasia Remizova, Arsenii Ashukha, Aleksei Silvestrov, Naejin Kong, Harshith Goka, Kiwoong Park, and Victor Lempitsky. 2022. Resolution-robust large mask inpainting with fourier convolutions. In *WACV*. 2149–2159.
- [118] Ying Tai, Jian Yang, and Xiaoming Liu. 2017. Image super-resolution via deep recursive residual network. In *CVPR*.
- [119] Xiaoou Tang and Xiaogang Wang. 2003. Face sketch synthesis and recognition. In *ICCV*.
- [120] Chunwei Tian, Lunke Fei, Wenxian Zheng, Yong Xu, Wangmeng Zuo, and Chia-Wen Lin. 2020. Deep learning on image denoising: An overview. *Neural Networks* (2020).
- [121] Lei Tian, Chunxiao Fan, Yue Ming, and Xiaopeng Hong. 2016. Weighted non-locally self-similarity sparse representation for face deblurring. In *ACCV*.
- [122] Anurag Singh Tomar, KV Arya, and Shyam Singh Rajput. 2023. Attentive ExFeat based deep generative adversarial network for noise robust face super-resolution. *PRL* 169 (2023), 58–66.
- [123] Anurag Singh Tomar, KV Arya, and Shyam Singh Rajput. 2023. Deep HyFeat Based Attention in Attention Model for Face Super-Resolution. *TIM* 72 (2023), 1–11.
- [124] Xiaoguang Tu, Jian Zhao, Qiankun Liu, Wenjie Ai, Guodong Guo, Zhifeng Li, Wei Liu, and Jiashi Feng. 2021. Joint face image restoration and frontalization for recognition. *TCSVT* (2021).
- [125] Naing Min Tun, Alexander I Gavrilov, and Nyan Linn Tun. 2020. Facial image denoising using convolutional autoencoder network. In *ICIEAM*. 1–5.
- [126] Ashish Vaswani, Noam Shazeer, Niki Parmar, Jakob Uszkoreit, Llion Jones, Aidan N Gomez, Łukasz Kaiser, and Illia Polosukhin. 2017. Attention is all you need. In *NeurIPS*.
- [127] Ziyu Wan, Bo Zhang, Dongdong Chen, Pan Zhang, Dong Chen, Jing Liao, and Fang Wen. 2020. Bringing old photos back to life. In *CVPR*.
- [128] Ziyu Wan, Bo Zhang, Dong Chen, Pan Zhang, Fang Wen, and Jing Liao. 2022. Old photo restoration via deep latent space translation. *TPAMI* 45, 2 (2022), 2071–2087.
- [129] Chenyang Wang, Junjun Jiang, Zhiwei Zhong, and Xianming Liu. 2023. Spatial-Frequency Mutual Learning for Face Super-Resolution. In *CVPR*. 22356–22366.
- [130] Jingkai Wang, Jue Gong, Lin Zhang, Zheng Chen, Xing Liu, Hong Gu, Yutong Liu, Yulun Zhang, and Xiaokang Yang. 2025. Osdface: One-step diffusion model for face restoration. In *CVPR*. 12626–12636.
- [131] Lingxiao Wang, Yali Li, and Shengjin Wang. 2017. DeepDeblur: fast one-step blurry face images restoration. *arXiv preprint arXiv:1711.09515* (2017).
- [132] Nannan Wang, Xinbo Gao, Dacheng Tao, and Xuelong Li. 2011. Face sketch-photo synthesis under multi-dictionary sparse representation framework. In *ICIG*.
- [133] Nannan Wang, Dacheng Tao, Xinbo Gao, Xuelong Li, and Jie Li. 2014. A comprehensive survey to face hallucination. *IJCV* (2014).
- [134] Wenhui Wang, Enze Xie, Xiang Li, Deng-Ping Fan, Kaitao Song, Ding Liang, Tong Lu, Ping Luo, and Ling Shao. 2021. Pyramid vision transformer: A versatile backbone for dense prediction without convolutions. In *ICCV*.
- [135] Xintao Wang, Yu Li, Honglun Zhang, and Ying Shan. 2021. Towards real-world blind face restoration with generative facial prior. In *CVPR*.
- [136] Xintao Wang, Ke Yu, Shixiang Wu, Jinjin Gu, Yihao Liu, Chao Dong, Yu Qiao, and Chen Change Loy. 2018. Esrgan: Enhanced super-resolution generative adversarial networks. In *ECCVW*.
- [137] Yu Wang, Tao Lu, Ruobo Xu, and Yanduo Zhang. 2020. Face super-resolution by learning multi-view texture compensation. In *MMM*.
- [138] Zhou Wang, Alan C Bovik, Hamid R Sheikh, and Eero P Simoncelli. 2004. Image quality assessment: from error visibility to structural similarity. *TIP* (2004).
- [139] Zhihao Wang, Jian Chen, and Steven CH Hoi. 2020. Deep learning for image super-resolution: A survey. *TPAMI* (2020).
- [140] Zhou Wang, Eero P Simoncelli, and Alan C Bovik. 2003. Multiscale structural similarity for image quality assessment. In *ACSSC*.
- [141] Zhouxia Wang, Jiawei Zhang, Runjian Chen, Wenping Wang, and Ping Luo. 2022. RestoreFormer: High-Quality Blind Face Restoration From Undegraded Key-Value Pairs. In *CVPR*.
- [142] Zhixin Wang, Ziyi Zhang, Xiaoyun Zhang, Huangjie Zheng, Mingyuan Zhou, Ya Zhang, and Yanfeng Wang. 2023. DR2: Diffusion-based Robust Degradation Remover for Blind Face Restoration. In *CVPR*. 1704–1713.
- [143] Feng Wei, Song Wang, Jucheng Yang, Xiao Sun, Yuan Wang, and Yarui Chen. 2023. A Composite Network Model for Face Super-Resolution with Multi-Order Head Attention Facial Priors. *PR* 139 (2023), 109503.
- [144] Yue Wu, Tal Hassner, KangGeon Kim, Gerard Medioni, and Prem Natarajan. 2017. Facial landmark detection with tweaked convolutional neural networks. *TPAMI* (2017).
- [145] Weihao Xia, Yujiu Yang, Jing-Hao Xue, and Baoyuan Wu. 2021. Towards open-world text-guided face image generation and manipulation. *arXiv preprint arXiv:2104.08910* (2021).

- [146] Hanyu Xiang, Qin Zou, Muhammad Ali Nawaz, Xianfeng Huang, Fan Zhang, and Hongkai Yu. 2023. Deep learning for image inpainting: A survey. *PR* 134 (2023), 109046.
- [147] Chengxing Xie, Qian Ning, Weisheng Dong, and Guangming Shi. 2023. TFRGAN: Leveraging Text Information for Blind Face Restoration With Extreme Degradation. In *CVPR*. 2534–2544.
- [148] Xiangyu Xu, Deqing Sun, Jinshan Pan, Yujin Zhang, Hanspeter Pfister, and Ming-Hsuan Yang. 2017. Learning to super-resolve blurry face and text images. In *ICCV*.
- [149] Lingbo Yang, Shanshe Wang, Siwei Ma, Wen Gao, Chang Liu, Pan Wang, and Peiran Ren. 2020. Hifacegan: Face renovation via collaborative suppression and replenishment. In *ACMMM*.
- [150] Tao Yang, Peiran Ren, Xuansong Xie, and Lei Zhang. 2021. Gan prior embedded network for blind face restoration in the wild. In *CVPR*.
- [151] Wenhan Yang, Robby T Tan, Shiqi Wang, Yuming Fang, and Jiaying Liu. 2020. Single image deraining: From model-based to data-driven and beyond. *TPAMI* (2020).
- [152] Wenming Yang, Xuechen Zhang, Yapeng Tian, Wei Wang, Jing-Hao Xue, and Qingmin Liao. 2019. Deep learning for single image super-resolution: A brief review. *TMM* (2019).
- [153] Yan Yang, Md Zakir Hossain, Tom Gedeon, and Shafin Rahman. 2022. S2FGAN: semantically aware interactive sketch-to-face translation. In *WACV*. 1269–1278.
- [154] Rajeev Yasarla, Federico Perazzi, and Vishal M Patel. 2020. Deblurring face images using uncertainty guided multi-stream semantic networks. *TIP* (2020).
- [155] Peng Ye, Jayant Kumar, Le Kang, and David Doermann. 2012. Unsupervised feature learning framework for no-reference image quality assessment. In *CVPR*.
- [156] Dong Yi, Zhen Lei, Shengcui Liao, and Stan Z Li. 2014. Learning face representation from scratch. *Computer Science* (2014).
- [157] Yu Yin, Joseph Robinson, Yulun Zhang, and Yun Fu. 2020. Joint super-resolution and alignment of tiny faces. In *AAAI*.
- [158] Jiahui Yu, Zhe Lin, Jimei Yang, Xiaohui Shen, Xin Lu, and Thomas S Huang. 2018. Generative image inpainting with contextual attention. In *CVPR*. 5505–5514.
- [159] Jun Yu, Baopeng Zhang, Zhengzhong Kuang, Dan Lin, and Jianping Fan. 2016. iPrivacy: image privacy protection by identifying sensitive objects via deep multi-task learning. *TIFS* (2016).
- [160] Wangbo Yu, Mingrui Zhu, Nannan Wang, Xiaoyu Wang, and Xinbo Gao. 2022. An Efficient Transformer Based on Global and Local Self-Attention for Face Photo-Sketch Synthesis. *TIP* 32 (2022), 483–495.
- [161] Xin Yu, Basura Fernando, Bernard Ghanem, Fatih Porikli, and Richard Hartley. 2018. Face super-resolution guided by facial component heatmaps. In *ECCV*.
- [162] Xin Yu and Fatih Porikli. 2016. Ultra-resolving face images by discriminative generative networks. In *ECCV*.
- [163] Xin Yu and Fatih Porikli. 2017. Face hallucination with tiny unaligned images by transformative discriminative neural networks. In *AAAI*.
- [164] Xin Yu and Fatih Porikli. 2017. Hallucinating very low-resolution unaligned and noisy face images by transformative discriminative autoencoders. In *CVPR*.
- [165] Yanjiang Yu, Puyang Zhang, Kaihao Zhang, Wenhan Luo, Changsheng Li, Ye Yuan, and Guoren Wang. 2022. Multi-Prior Learning via Neural Architecture Search for Blind Face Restoration. *arXiv preprint arXiv:2206.13962* (2022).
- [166] Zongsheng Yue and Chen Change Loy. 2024. Difface: Blind face restoration with diffused error contraction. *IEEE Transactions on Pattern Analysis and Machine Intelligence* (2024).
- [167] Zongsheng Yue, Hongwei Yong, Qian Zhao, Deyu Meng, and Lei Zhang. 2019. Variational denoising network: Toward blind noise modeling and removal. In *NeurIPS*.
- [168] Stefanos Zafeiriou, George Trigeorgis, Grigoris Chrysos, Jiankang Deng, and Jie Shen. 2017. The menpo facial landmark localisation challenge: A step towards the solution. In *CVPRW*.
- [169] Kangli Zeng, Zhongyuan Wang, Tao Lu, Jianyu Chen, Jiaming Wang, and Zixiang Xiong. 2023. Self-attention learning network for face super-resolution. *NN* 160 (2023), 164–174.
- [170] Kangli Zeng, Zhongyuan Wang, Tao Luz, Jianyu Chen, Zheng He, and Zhen Han. 2024. Implicit Mutual Learning With Dual-Branch Networks for Face Super-Resolution. *TBBIS* (2024).
- [171] Kaihao Zhang, Dongxu Li, Wenhan Luo, Jingyu Liu, Jiankang Deng, Wei Liu, and Stefanos Zafeiriou. 2022. EDFace-Celeb-1 M: Benchmarking Face Hallucination with a Million-scale Dataset. *TPAMI* (2022).
- [172] Kaihao Zhang, Wenhan Luo, Yiran Zhong, Lin Ma, Bjorn Stenger, Wei Liu, and Hongdong Li. 2020. Deblurring by realistic blurring. In *CVPR*.
- [173] Kaihao Zhang, Wenqi Ren, Wenhan Luo, Wei-Sheng Lai, Björn Stenger, Ming-Hsuan Yang, and Hongdong Li. 2022. Deep image deblurring: A survey. *IJCV* (2022).
- [174] Kaipeng Zhang, Zhanpeng Zhang, Chia-Wen Cheng, Winston H Hsu, Yu Qiao, Wei Liu, and Tong Zhang. 2018. Super-identity convolutional neural network for face hallucination. In *ECCV*.
- [175] Puyang Zhang, Kaihao Zhang, Wenhan Luo, Changsheng Li, and Guoren Wang. 2022. Blind Face Restoration: Benchmark Datasets and a Baseline Model. *arXiv preprint arXiv:2206.03697* (2022).
- [176] Richard Zhang, Phillip Isola, Alexei A Efros, Eli Shechtman, and Oliver Wang. 2018. The unreasonable effectiveness of deep features as a perceptual metric. In *CVPR*.

- [177] Tianyu Zhao and Changqing Zhang. 2020. Saan: Semantic attention adaptation network for face super-resolution. In *ICME*.
- [178] Yang Zhao, Tingbo Hou, Yu-Chuan Su, Xuhui Jia Li, Matthias Grundmann, et al. 2023. Towards Authentic Face Restoration with Iterative Diffusion Models and Beyond. *arXiv preprint arXiv:2307.08996* (2023).
- [179] Yang Zhao, Yu-Chuan Su, Chun-Te Chu, Yandong Li, Marius Renn, Yukun Zhu, Changyou Chen, and Xuhui Jia. 2022. Rethinking Deep Face Restoration. In *CVPR*.
- [180] Erjin Zhou, Haoqiang Fan, Zhimin Cao, Yuning Jiang, and Qi Yin. 2015. Learning face hallucination in the wild. In *AAAI*.
- [181] Shangchen Zhou, Kelvin Chan, Chongyi Li, and Chen Change Loy. 2022. Towards robust blind face restoration with codebook lookup transformer. In *NIPS*. 30599–30611.
- [182] Feida Zhu, Junwei Zhu, Wenqing Chu, Xinyi Zhang, Xiaozhong Ji, Chengjie Wang, and Ying Tai. 2022. Blind Face Restoration via Integrating Face Shape and Generative Priors. In *CVPR*.
- [183] Mingrui Zhu, Changcheng Liang, Nannan Wang, Xiaoyu Wang, Zhifeng Li, and Xinbo Gao. 2021. A Sketch-Transformer Network for Face Photo-Sketch Synthesis.. In *IJCAI*.
- [184] Shizhan Zhu, Sifei Liu, Chen Change Loy, and Xiaoou Tang. 2016. Deep cascaded bi-network for face hallucination. In *ECCV*.
- [185] Xiangyu Zhu, Zhen Lei, Xiaoming Liu, Hailin Shi, and Stan Z Li. 2016. Face alignment across large poses: A 3d solution. In *CVPR*.